

RNA G-quadruplexes in Kirsten ras (*KRAS*) oncogene as targets for small molecules inhibiting translation

Giulia Miglietta, Susanna Cogoi, Jessica Marinello, Giovanni Capranico, Alexander S. Tikhomirov, Andrey E. Shchekotikhin, and Luigi E. Xodo

J. Med. Chem., **Just Accepted Manuscript** • Publication Date (Web): 15 Nov 2017

Downloaded from <http://pubs.acs.org> on November 15, 2017

Just Accepted

“Just Accepted” manuscripts have been peer-reviewed and accepted for publication. They are posted online prior to technical editing, formatting for publication and author proofing. The American Chemical Society provides “Just Accepted” as a free service to the research community to expedite the dissemination of scientific material as soon as possible after acceptance. “Just Accepted” manuscripts appear in full in PDF format accompanied by an HTML abstract. “Just Accepted” manuscripts have been fully peer reviewed, but should not be considered the official version of record. They are accessible to all readers and citable by the Digital Object Identifier (DOI®). “Just Accepted” is an optional service offered to authors. Therefore, the “Just Accepted” Web site may not include all articles that will be published in the journal. After a manuscript is technically edited and formatted, it will be removed from the “Just Accepted” Web site and published as an ASAP article. Note that technical editing may introduce minor changes to the manuscript text and/or graphics which could affect content, and all legal disclaimers and ethical guidelines that apply to the journal pertain. ACS cannot be held responsible for errors or consequences arising from the use of information contained in these “Just Accepted” manuscripts.

RNA G-quadruplexes in Kirsten ras (*KRAS*) oncogene as targets for small molecules inhibiting translation

Giulia Miglietta,¹ Susanna Cogo,¹ Jessica Marinello,² Giovanni Capranico,² Alexander S. Tikhomirov,³ Andrey Shchekotikhin,³ Luigi E. Xodo^{1*}

¹ Department of Medical and Biological Sciences, University of Udine, 33100 Udine, Italy;

² Department of Pharmacy and Biotechnology, University of Bologna,

40100 Bologna, Italy;

³ Gause Institute of New Antibiotics, 119 021 Moscow, Russia;

KEYWORDS: *KRAS*, 5'-UTR, RNA G-quadruplexes, anthrafurandione, anthrathiophenedione, translation inhibition, Panc-1 cells, apoptosis.

ABSTRACT

The human *KRAS* transcript contains a G-rich 5'-UTR sequence (77 % GC) harbouring several G4 motifs capable to form stable RNA G-quadruplex (RG4) structures that can serve as targets for small molecules. A biotin-streptavidin pull-down assay showed that 4,11-bis(2-aminoethylamino)anthra[2,3-*b*]furan-5,10-dione (**2a**) binds to RG4s in the *KRAS* transcript under low-abundance cellular conditions. Dual-luciferase assays demonstrated that **2a** and its analogue 4,11-bis(2-aminoethylamino)anthra[2,3-*b*]thiophene-5,10-dione (**2b**) repress translation in a dose-dependent manner. The effect of the G4-ligands on Panc-1

1
2
3 cancer cells has also been examined. Both **2a** and **2b** efficiently penetrate the cells
4
5 suppressing protein p21KRAS to < 10 % of the control. The *KRAS* down-regulation induces
6
7 apoptosis together with a dramatic reduction of cell growth and colony formation. In
8
9 summary, we report a strategy to suppress the *KRAS* oncogene in pancreatic cancer cells by
10
11 means of small molecules binding to RG4s in the 5'-UTR of mRNA.
12
13
14

15 INTRODUCTION

16
17 The three ras genes (*HRAS*, *KRAS* and *NRAS*) encode for highly homologous (83-90 %
18
19 sequence identity) GTPases of 21 kDa that cycle between an active GTP-bound and an
20
21 inactive GDP-bound state.^{1,2} This cycling is mediated by guanine nucleotides exchange
22
23 factors (GEFs) and by GTPases activating proteins (GAPs).^{1,3} In the GTP-bound state, the
24
25 p21RAS protein interacts with downstream effectors, activating specific cellular processes
26
27 including proliferation, survival and differentiation.^{3,4} Mutations in the ras genes are
28
29 estimated to be present in ~ 30 % of all human cancers.⁵ However, in pancreatic ductal
30
31 adenocarcinoma (PDAC), *KRAS* is mutated in ~ 95 % of patients.^{6,7} The mutant alleles
32
33 carry a single missense point mutation in exon 1, codon 12, 13 or 61, which impairs GAP-
34
35 mediated GTP-to-GDP hydrolysis. This results in an aberrant protein that is locked into the
36
37 activated state, transmitting constitutively signals for proliferation to the nucleus.⁸
38
39 According to recent studies, mutations in the *KRAS* gene can be seen as primary genetic
40
41 lesions that initiate the malignant transformation of pancreatic cells.^{9,10} Progression to
42
43 invasive PDAC occurs through a step-wise accumulation of other genetic lesions, in
44
45 particular those causing the inactivation of tumour suppressor genes.¹¹
46
47
48
49

50 Recent studies have demonstrated that *KRAS* is essential for the maintenance of PDAC
51
52 as it reprograms the metabolism of glucose and glutamine to fuel a high proliferation rate.⁹
53
54 ^{12, 13} The dependence of metabolic pathways on specific oncogenes has led to the concept of
55
56
57
58
59
60

1
2
3 “oncogene addiction”, which means that, although cancer cells may depend on a number of
4 genetic aberrations, they often develop a dependency on a particular oncogene.^{14, 15}
5
6 Considering the central role played by *KRAS* on the pathogenesis of PDAC, *KRAS* is
7 considered a crucial target for anticancer drugs. However, despite more than two decades of
8 research, up to now no anti-ras drugs have reached the clinic, creating the impression that
9 ras genes may be “undruggable”.^{16, 17} Recently, the design of new inhibitors binding
10 directly to protein p21RAS has fuelled research in this direction.¹⁸ Other strategies that are
11 being pursued use drugs that inhibit either the association of p21RAS to the membrane or
12 the activity of downstream pathways.¹⁹⁻²² In our laboratory, we developed an alternative
13 anti *KRAS* strategy by focusing on two targets for small molecules: (i) a G4-motif located
14 upstream of the transcription start site (TSS) (-320/-306), which is recognized by essential
15 transcription factors (MAZ, Ku70, PARP-1 and hnRNP A1);²³ (ii) G4-motifs located in the
16 5'-untranslated region (5'-UTR) of the *KRAS* transcript.^{24, 25} Previous studies have shown
17 that the presence of G4 motifs in 5'-UTR of mRNA inhibits translation, on the basis of
18 luciferase assays.^{26, 27} In this study, we demonstrate by a streptavidin-biotin pull-down
19 assay that small molecules bind to RNA G-quadruplexes (RG4s) formed in the 5'-UTR of
20 low-abundant cellular *KRAS* transcripts. These small molecules, anthrafurandiones (ATFD)
21 and anthrathiophenediones (ATPD), suppress luciferase from specific vectors as well as
22 p21RAS in pancreatic Panc-1 cancer cells. ATFD and ATPD strongly induce apoptosis,
23 reduce the metabolic activity and colony formation of Panc-1 cells carrying mutant *KRAS*
24 G12D. Our results demonstrate that ATPD and ATFD are promising therapeutic drugs to
25 suppress oncogenic *KRAS* in pancreatic cancer cells, through their binding to RG4s located
26 in the 5'-UTR of mRNA.
27
28
29
30
31
32
33
34
35
36
37
38
39
40
41
42
43
44
45
46
47
48
49
50
51
52
53
54
55
56
57
58
59
60

RESULTS AND DISCUSSION

Since Hurley and co-workers published their seminal study on the transcription of *CMYC* controlled by a regulatory mechanism involving a G4 DNA,²⁸ a great number of papers on this unusual structure has been reported in the literature.²⁹⁻³⁵ The biological function of G4 DNA is rather complex: some studies indicate that it behaves as a transcriptional repressor,^{28,32,35} others that G4 DNA is associated with transcriptionally-active chromatin.³⁶ Whatever its function is, G4 DNA is an attractive target for therapeutic small molecules.³² However, bioinformatics analyses showed that the transcript of certain oncogenes contains a 5'-UTR rich in guanines that can form G4 RNA structures (RG4s).^{26,27,37-40} The 5'-UTR region of mRNA plays an essential role in the initiation of translation. This occurs through three steps: (i) association of the 7-methylguanosine cap with the 43 S initiation complex; (ii) scanning of complex 43 S along 5'-UTR up to codon AUG; (iii) assembly of a larger 80 S ribosome that proceeds with protein synthesis. The process is normally regulated by eukaryotic translation initiation factors (eIFs). In addition, certain transcripts use a cap-independent translation initiation that depends on internal ribosomal entry sites.^{26,39,40} It has been hypothesized that excess secondary structure including RG4s, in 5'-UTR may have a regulatory function on translation.^{26,27,37-40} Indeed, as observed with RNA hairpins, RG4s can either inhibit the assembly of the translation initiation machinery at the 5'-cap or interfere with the scanning of the ribosome towards the AUG codon (Supp. data, S1).^{26,41-47} Luciferase data obtained with expression plasmids designed with G4 in specific positions upstream of AUG have been reported as a proof-of-principle.^{26,43,44} In our work we demonstrate that furan- and thiophene-fused anthraquinone derivatives bind to RG4s in the 5'-UTR of *KRAS* mRNA under low-abundance cellular conditions. These G4-specific molecules are found to suppress the *KRAS* oncogene in pancreatic cancer cells through a mechanism involving the inhibition of translation.

The human *KRAS* 5'-UTR forms RNA G-quadruplex structures

The human *KRAS* transcript contains a 5'-UTR of 192 nucleotides, characterized by a high GC content (77 %) (Fig. 1). Its putative secondary structure can be predicted by Mfold,⁴⁸ a bioinformatic tool that generates a secondary structure by taking into consideration the orthologues of the RNA sequence. However, Mfold does not take into account G4 motifs, thus one wonders if the secondary structure predicted for the *KRAS* 5'-UTR is actually formed, considering that it contains 33 GG runs which give rise to a multitude of G4 motifs. To identify the G4 motifs with the highest G-score (i.e. highest propensity to fold into a G4), we interrogated QGRS Mapper.⁴⁹ We considered a consensus G4 motif composed by 2 G-tetrads and loop length up to 12 nt. The analysis gave three non-overlapping G4 motifs with a G-score= 21 (Table 1). If the overlapping G4 motifs were included in the analysis, their number was > 300, suggesting that the human *KRAS* 5'-UTR sequence has a high propensity to form RG4s. The three non-overlapping G4 motifs are located within the first 80 nt of 5'-UTR and each displays a circular dichroism spectrum characterized by a strong ellipticity at 265 nm and a negative ellipticity at 240 nm, typical of parallel G-quadruplexes, as does the well-known G4-motif located in the 5'-UTR of *NRAS* (Fig. 2 A).^{26,50} The G4 motifs show UV-thermal difference spectra characterized by a negative peak at 295 nm in K⁺- but not in Li⁺-buffer, a distinctive feature of G4 structures (Supp. data, S2).⁵¹ They show cooperative UV-melting curves at 296 nm (as well as at 260 nm), with T_M varying from 53 to 64 °C in K⁺-buffer (Fig. 2 B and Table 1). The melting curves analysed with a two-state model, gave ΔG of quadruplex formation between ~ -3.7 and -5.6 kcal/mol (Table 1).

To confirm that the selected G4 motifs adopt a RG4 structure, we analysed by EMSA if they are recognized by BG4, an antibody specific for G-quadruplexes.^{52,53} This analysis was performed with only the 20-mer *utr-z* G4 motif, as *utr-1* and *utr-c* are too short for

1
2
3 binding to BG4. We found that BG4 formed a stable RNA-protein complex with *utr-z* as
4 well as with the *NRAS* RG4, which was used as a positive control (Fig. 2 C).²⁶ Next, we
5 analysed by EMSA the first 80-nt of 5'-UTR (s-80), which contains the three non-
6 overlapping G4 motifs. We wanted to find out if the G4 structures are also present in this
7 longer RNA s-80 sequence, although it could form a mismatched stem-loop structure,
8 according to Mfold (Fig. 3 A). We found that in K⁺-buffer, BG4 clearly bound to s-80,
9 while it did not essentially bind to single-stranded RNA or hairpin RNA sequences, thus
10 suggesting that *KRAS* 5'-UTR forms indeed local G4 structures (Fig. 3 B). We found that
11 BG4 bound to s-80, although with a weaker intensity, also in Li⁺-buffer. This is probably
12 due to the fact that s-80 exists as a hairpin=G4 equilibrium, which is more shifted to the
13 right in K⁺- than Li⁺-buffer. BG4, upon binding to the existing quadruplex, is likely to push
14 the equilibrium to the right. The capacity of RNA sequences to fold into G4s in the absence
15 and presence of various metal ions, including K⁺, Na⁺ and Li⁺, has been examined by
16 Miserachs et al.⁵⁴ Further evidence that G4 is present in s-80 was obtained by measuring
17 the reactivity of the guanines with RNase T1,⁵⁵ taking into account that the guanines
18 involved in the formation of Watson-Crick or Hoogsteen hydrogen bonds do not react with
19 RNase T1. If s-80 assumes the stem-loop structure of Fig. 3 A, the loop guanines G23-G24
20 and G26-G27 should be reactive. On the other hand, if s-80 forms the three non-overlapping
21 G4 structures, the loop guanines should not be reactive, as they should be involved in the
22 formation of the G-tetrads. In contrast, guanines G30 and G33, falling between the *utr-l*
23 and *utr-z* RG4 structures, should be reactive to RNase T1. The footprinting of s-80 over the
24 loop region shows that there is a prevalence of stem-loop structure in Li⁺-buffer as G30 and
25 G33 are not or very slightly reactive (Fig. 3 C, from left lanes 4 and 7). By contrast, in K⁺-
26 buffer both G4 and stem-loop structures are present in solution, as G30 and G33 as well as
27 G23-G24 and G26-G27 are clearly reactive with RNase T1 (lanes 3 and 6 from left). This
28
29
30
31
32
33
34
35
36
37
38
39
40
41
42
43
44
45
46
47
48
49
50
51
52
53
54
55
56
57
58
59
60

behaviour suggests that s-80 exists in solution in equilibrium between G4 and the stem-loop structure. To further support this conclusion, we tested the presence of RG4s in s-80 with thioflavin T (ThT), a fluorescence sensor specific for G4.⁵⁶ As illustrated in Fig. 4A, ThT exhibited a strong increase of fluorescence emission upon binding to s-80, but not upon binding to a RNA hairpin (5'-GGCCGCCGCAGUGGCGGCGG). In Fig. 4B we compared the fluorescence enhancement of ThT induced by s-80 or hairpin RNA, in K⁺- or Li⁺-buffer.

It can be seen that in K⁺-buffer s-80 caused an increase of fluorescence (F/F₀) up to 25 while in Li⁺-buffer only up to 10, in agreement with the fact that the hairpin = G4 equilibrium is more shifted to the right in the K⁺-buffer. By comparison, a designed hairpin RNA increases F/F₀ up to 5. These data strongly suggest that under physiological conditions, RG4 structures are certainly present in the first portion of *KRAS* 5'-UTR. Recently, Weldon et al.⁵⁷ performed RNA footprintings on wild-type Bcl-x-681 transcript and its 7-deaza-G analogue, which cannot form RG4. They found that RG4 is present in the transcript, despite a possible formation of competing stem-loop structures. The Bcl-x G4 motifs have G-scores similar or lower ($15 \leq \text{G-score} \leq 21$) than those found in the 5'-UTR of *KRAS* (G-score= 21)

ATPD and ATFD: uptake and capacity to stabilize RG4

As the 5'-UTR of *KRAS* is conserved in mammals (Supp. data, S3) and forms RG4s, we hypothesized that these unusual structures could be involved in the mechanism regulating translation of *KRAS*. Previous studies have showed that translation can be modulated by small molecules targeting to RG4s.^{41, 58, 59} We therefore searched for molecules that obey the following criteria: (i) high capacity to penetrate cell membranes; (ii) binding to *KRAS* mRNA despite its typical cellular low-abundance; (iii) high affinity for RG4s. In previous studies we reported that anthrathiophenediones (ATPD) with alkyl side-

1
2
3 chains carrying either guanidine or chloroacetamide terminal groups penetrate bladder
4
5 cancer cells and bind to DNA and RNA G4s.^{60,61} Since the side chains strongly impact the
6
7 uptake of these molecules,⁶⁰ we tested in human pancreatic Panc-1 cancer cells several
8
9 ATPD analogues and focused on 4,11-bis[2-guanidinoethylamino)anthra[2,3-*b*]thiophene-
10
11 5,10-dione (**1b**), 4,11-bis(2-aminoethylamino)anthra[2,3-*b*]thiophene-5,10-dione (**2b**)⁶² as
12
13 well as on their furan analogues, anthrafurandiones (ATFD) **1a** and **2a**⁶³ (Fig. 5 A). Both
14
15 types of ligands have alkyl side chains ending either with guanidine or amine groups. As the
16
17 chromophore of these molecules emits fluorescence upon excitation at 488 nm, we
18
19 investigated their cellular uptake by FACS (Fig. 5 B). The results showed that compounds
20
21 **2a** and **2b** with amino-ethyl side chains are taken up 20- and 4-fold more efficiently than
22
23 the corresponding guanidine analogues **1a** and **1b**, respectively. An explanation can be that
24
25 compounds carrying a localized charge generally display lower membrane permeability
26
27 than neutral compounds. Compound **2a** differs from **2b** only for an atom in the 5-member
28
29 ring: oxygen against sulfur. Nonetheless, the former is 5-fold more permeable to Panc-1
30
31 cells than the latter. The higher polarizability of sulfur compared to oxygen provides a
32
33 rationale for this behaviour.⁶⁴ Due to their high uptake in Panc-1 cells, we used **2a** and **2b**
34
35 to design a strategy aiming at inhibiting translation of *KRAS* in Panc-1 cells. The guanidine
36
37 analogues **1a** and **1b** were used as reference compounds: since their uptake is lower, they
38
39 are expected to produce a weaker cellular effect. We first asked if the molecules bind to and
40
41 stabilize the RG4 structures. UV-melting experiments showed that **2a** and, to a less extent,
42
43 **2b** strongly stabilize the three non-overlapping RG4s located in the *KRAS* 5'-UTR. The
44
45 increase of T_M (ΔT_M) of the three RG4s in the presence of the G4 ligands at $r=1, 2$ and 4 (r
46
47 = [ligand]/[G4]) are reported in the histograms of Fig. 5 C. It can be seen that **2a** caused a
48
49 T_M increase up to 32 °C, while **2b** up to 20 °C. The lower ΔT_M brought about by **2b** is
50
51 probably due to the polarizability of sulfur that may reduce the stacking of the chromophore
52
53
54
55
56
57
58
59
60

1
2
3 upon the G-tetrads. Our data show that when thiophene is replaced with furan, the ligand
4 increases not only its capacity to stabilize RG4 but also the uptake in Panc-1 cells. We also
5 investigated the quadruplex-to-duplex specificity of the G4 ligands by competition
6
7 experiments. For instance, the T_M of *utr-1* RG4 in the presence of **2a** at $r=4$ did not change
8
9 when a 5- or 10-fold excess 21-mer RNA duplex was added to the mixtures (not shown).
10
11
12

13 This is in keeping with our previously data on analogue ligands.^{60,61}

14
15 Finally, the affinity of ligands **2a** and **2b** for various G4 RNAs located in 5'-UTR was
16 determined by fluorescence titrations. A typical titration obtained with *utr-1* and **2a** is
17 shown in Supp. data S4. The various K_D 's are reported in Table 2. It can be seen that the
18 average K_D values for **2a** is ~ 140 nM and for **2b** is ~ 156 nM. The K_D for the binding of the
19 ligands to competing mismatched hairpin RNAs could not be measured as we were unable
20 to find experimental conditions in which these putative structures, predicted by Mfold, are
21 stable. We also designed a non-natural RNA stem-loop structure and found that **2a** and **2b**
22 have affinities for this hairpin from 2 to 6 times lower than that for the RG4s. Interestingly,
23 the K_D 's for the binding of the ligands to the critical G4 DNA formed in the *KRAS* promoter
24 are 626 ± 71 nM for **2a** and 278 ± 21 nM for **2b**. Although the ligands can bind also to G4
25 DNA, the fact that they accumulate more in the cytoplasm than in the nucleus (Supp. data
26 S5) and that there are many copies of mRNA RG4s, suggest that the main targets, i.e. those
27 producing a stronger cellular effect, is likely to be in mRNA.
28
29
30
31
32
33
34
35
36
37
38
39
40
41
42
43
44
45
46

47 **ATFDs target the *KRAS* transcript under cellular low abundance conditions**

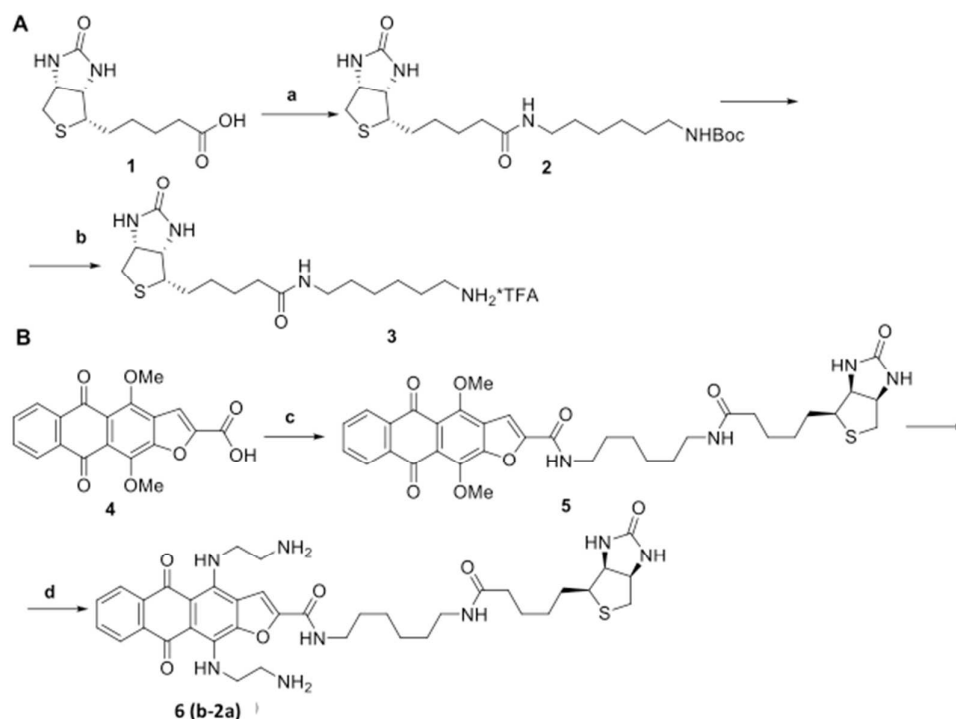
48
49 Studies so far reported on the use of small molecules to inhibit translation are based on
50 luciferase assays and on the assumption that the G4 ligands bind to mRNA.^{26,43-45} The first
51 issue that we addressed in our study was to demonstrate that **2a** (the compound showing the
52 highest uptake) does indeed bind to *KRAS* mRNA, under its low-abundance cellular
53
54
55
56
57
58
59
60

1
2
3 condition. To do this, we synthesized biotinylated **2a** (**b-2a**) and set up a biotin-streptavidin
4
5 pull-down assay.

6
7 **Synthesis of biotinylated 2a (b-2a).** The synthesis of compounds **1a** and **1b**, **2a**, **2b**, based
8
9 on the nucleophilic substitution of alkoxy groups in the *peri*-positions of heteroarene-fused
10
11 anthracenediones, has been described previously.⁶²⁻⁶⁵

12
13 To link biotin to **2a** we used as spacer 1,6-diaminohexane.⁶⁶⁻⁶⁸ First, biotin (**1**) was coupled
14
15 with mono-Boc-protected 1,6-diaminohexane using HATU as coupling reagent. The
16
17 subsequent cleavage of the protecting group led to building block HDA-Biotin (**3**) (Scheme
18
19 1A).⁶⁶ As starting compound for the biotinylation of **2a** we used 4,11-dimethoxy-5,10-
20
21 dioxoanthra[2,3-*b*]furan-2-carboxylic acid (**4**).⁶⁹ The condensation of the amine group of **3**
22
23 with the carboxylic group of **4** in presence of PyBOP yielded the
24
25

26
27 **Scheme 1.** Synthesis of biotinylated anthrafurandiones **b-2a**



1
2
3 Reagents and conditions: (a) BocNH(CH₂)₆NH₂, HATU, NMM, DMF, rt; overnight; yield
4 89 %; (b) DCM, TFA, rt; 3 h; yield 87 %; (c) **3**, PyBOP, DIPEA, DMSO, rt, 1 h, yield 80
5 %; (d) ethylenediamine, THF, 50 °C, 1.5–2 h, yield 68 %.

6
7
8
9
10
11 biotinylated 4,11-dimethoxy intermediate **5** (Scheme 1B). Finally, by treating 4,11-
12 dimethoxyanthra[2,3-*b*]furan-2-carboxamide (**5**) with ethylenediamine in THF at 50 °C we
13 obtained to biotinylated 4,11-bis(aminoalkylamino)anthra[2,3-*b*]furan-5,10-dione **6 (b-2a)**.

14
15
16
17
18
19 ***Streptavidin-biotin pull-down assays with b-2a.*** To demonstrate that the ligands bind to
20 RG4s in *KRAS* mRNA, we first ask if, by means of a biotin-streptavidin assay, **b-2a** is
21 capable to pull down a DNA containing a G4 structure. We designed two DNA strands of
22 115 and 89 nt of which the former contained in the middle a G4 motif (telomeric *htel*⁷⁰).
23
24 Both DNA strands had the same 5'- and 3'-ends and could be amplified with the same
25 couple of primers. A 1:1 mixture of the two strands was incubated with an excess **b-2a** and
26 the DNA bound to the biotinylated ligand was pulled down by streptavidin-magnetic beads
27 and the recovered DNA amplified. On a calibration curve, the DNA recovered was
28 dramatically enriched of the 115-nt sequence containing G4, suggesting that **b-2a** efficiently
29 pulled down the DNA strand carrying G4: a prerequisite essential for the next step of the
30 experiment. (Supp. data, S6).

31
32
33
34
35
36
37
38
39
40
41
42
43 The pull-down experiment was repeated by replacing the 1:1 mixture with total cellular
44 RNA extracted from Panc-1 cells. Cellular RNA is composed by ribosomal, transfer and, in
45 minimal part, messenger RNA. As illustrated in Fig. 6B the transcriptome contains mRNAs
46 without G4 structures (like HPRT) and with G4 structures in 5'-UTR as *KRAS*. We
47
48 reasoned that while all transcripts will have weak binding sites for **b-2a** (RNA stem-loop
49 secondary structures), only a fraction of transcripts will exhibit both weak (stem-loop) and
50
51
52
53
54
55
56
57
58
59
60

1
2
3 strong (G4) binding sites for b-**2a**. Based on this assumption, total cellular RNA from Panc-
4
5 1 cells was incubated with b-**2a** and the RNA bound to the ligand was pulled down with
6
7 streptavidin-coated magnetic beads. The amounts of *KRAS* and HPRT transcripts in the
8
9 recovered RNA were determined by quantitative RT-PCR and compared to the amounts of
10
11 the same genes detected in the input (untreated cellular RNA). The results showed that
12
13 *KRAS*/HPRT in the pulled-down RNA increased nearly 3-fold compared to the input,
14
15 suggesting that b-**2a** binds indeed to RG4s in *KRAS* transcripts. The pull-down experiment
16
17 was repeated with increasing concentrations of b-**2a** (from 400 to 800 nM). The highest
18
19 enrichment in *KRAS* transcript was obtained at a concentration of **2a** of 600 nM. With
20
21 higher concentrations of b-**2a**, the enrichment decreased as the ligand bound to both strong
22
23 (G4) and weak (stem-loop) sites (Fig. 6B). Together, the data demonstrate that a small
24
25 molecule such as **2a**, designed to inhibit gene expression, targets G4 RNA in the 5'-UTR of
26
27 the *KRAS* transcript under cellular conditions in which the transcript is typically low
28
29 abundant.
30
31
32
33
34

35 **Capacity of compounds 2a and 2b to repress translation in pancreatic cancer cells**

36
37 After having demonstrated that ATPD and ATFD bind to RG4s in the *KRAS* transcript,
38
39 we asked if they inhibit the translation of the oncogene in pancreatic cancer cells. First, we
40
41 performed a dual-luciferase assay as a proof-of-principle. We used a plasmid where *Renilla*
42
43 luciferase was driven by the *KRAS* promoter including 5'-UTR (pRL-KRAS). To determine
44
45 the transfection efficiency, we used pHRAS-mutA-luc, in which *Firefly* luciferase is driven
46
47 by a mutated *HRAS* promoter, which does not bear G4 motifs (Fig. 7 A).⁷¹ Panc-1 cells
48
49 were first treated for 6 h with increasing amounts of **2a**, **2b** and with the guanidine
50
51 analogues **1a** and **1b** (from 0.3 to 1.6 μ M), then with the luciferase vectors. The ratio
52
53 between *Renilla* and *Firefly* luciferases was measured 48 h after transfection. It can be seen
54
55
56
57
58
59
60

1
2
3 that **2a** and **2b** at concentrations between 0.3 and 1.6 μM dramatically lower luciferase,
4
5 much more than the reference guanidine analogues (Fig. 7 B). When **2a** was used at lower
6
7 concentrations, between 0.07 and 0.33 μM , a clear dose-response inhibitory effect was
8
9 observed (Fig. 7 C). If one considers that the four ligands have similar affinity for *utr-z* (and
10
11 also for the other RG4s) but different uptake in Panc-1 cells, there is a clear correlation
12
13 between luciferase inhibition and uptake. The higher the uptake (**2a** and **2b**), the higher the
14
15 luciferase inhibition”

16
17
18 It might be argued that the luciferase repression mediated by **2a** and **2b** is due to the
19
20 binding of the ligands not only to the RG4s in 5'-UTR but also to G4 in the *KRAS*
21
22 promoter.^{23, 72, 73} To address this point, we prepared a vector where *Renilla* luciferase is
23
24 driven by the cytomegalovirus (CMV) promoter. At the 3'-end of CMV promoter we
25
26 inserted the *KRAS* 5'-UTR (pRL-CMV-UTR). As the CMV promoter does not form G4
27
28 structures, the strong binding sites for **2a** are only located in the 5'-UTR sequence. As a
29
30 reference vector we used pHRAS-mutA-luc. The dual luciferase assay showed that **2a**
31
32 represses *Renilla* luciferase expression in a dose response manner, suggesting that the
33
34 presence of *KRAS* 5'-UTR alone is sufficient to promote the repression of luciferase. (Fig.
35
36 8, left panel). The inhibition is observed with higher ligand concentrations than those used
37
38 with plasmid pRL-KRAS, because the CMV promoter is stronger than the *KRAS* promoter.
39
40 We then measured the effect of **2a** on pRL-CMV, which lacks the *KRAS* 5'-UTR
41
42 downstream of the CMV promoter. In this case **2a** did not repress *Renilla* luciferase, in
43
44 agreement with the fact that G4 is not present in this construct (Fig. 8, right panel). This
45
46 experiment supports the conclusion that **2a** upon binding to RG4 in the 5'-UTR of *KRAS*
47
48 inhibits translation. We cannot rule out that the compounds also bind to the *KRAS* promoter.
49
50 However, considering that: (i) the G4 ligands accumulate more in the cytoplasm than in the
51
52 nucleus (Supp. data, S5); (ii) there are many copies of RNA targets in the cells, even under
53
54
55
56
57
58
59
60

1
2
3 mRNA low-abundance cellular conditions, **2a** and **2b** are expected to bind more favourably
4
5 to G4 in mRNA than in promoter DNA.
6
7

9 **Effect of 2a and 2b on *KRAS* expression in pancreatic cancer cells**

10
11 As the designed compounds, in particular **2a**, decrease the luciferase from vectors
12
13 containing the *KRAS* 5'-UTR, we asked if these G4 ligands are also able to inhibit the
14
15 expression of genomic *KRAS* in pancreatic cancer cells. We measured by quantitative RT-
16
17 PCR the level of *KRAS* transcript in Panc-1 cells after 6 and 24 h of treatment. The results
18
19 showed that while **2b**, **1a** and **1b** did not lower the level of mRNA, **2a** reduced it to about
20
21 50 % of the control, at both time points. By contrast, all the compounds displayed a strong
22
23 capacity to suppress the *KRAS* protein. In particular **2a** and **2b**, which are efficiently taken
24
25 up by Panc-1 cells, brought the protein down to < 10 % of the control (Fig. 9 A, B). In the
26
27 light of these results we concluded that **2a** and **2b** inhibit *KRAS* mainly at translational
28
29 level. Moreover, both luciferase and western blot data show that compound **2a** is slightly
30
31 more active than **2b**; possibly because **2a** has a higher capacity to penetrate cell membrane
32
33 than **2b**, and a fraction of it may also target G4 in the *KRAS* promoter.
34
35
36

37
38 Pancreatic cancer cells, being addicted to *KRAS*, respond to the repression of the
39
40 oncogene by activating apoptosis.⁷⁴ We found indeed that **2a** and to a lesser extent **2b**
41
42 caused a strong activation of caspases 3/7 (Fig. 10 A). In contrast, the reference compounds
43
44 **1a** and **1b** showed a much weaker caspase activation. To confirm the activation of apoptosis
45
46 we also performed an annexin/propidium iodide assay (Fig. 10 B). This is based on the
47
48 observation that an early event occurring in apoptosis is the translocation of
49
50 phosphatidylserine from the inner to the outer leaflet of the plasma membrane, thus
51
52 exposing the phospholipid to the external cell environment. Annexin V, a
53
54 phosphatidylserine recognizing protein labeled with FITC, can be used to detect this event
55
56
57
58
59
60

1
2
3 by FACS. Early and late apoptosis can be distinguished by using both annexin V and
4 propidium iodide (PI).⁷⁵ The experiment showed that 1.6 μM **2a** and **2b** increased the
5 population of apoptotic cells 72 h after treatment: untreated Panc-1 cells (apoptotic cells ~
6 1.2 %); Panc-1 cells treated with **2a** (apoptotic cells ~ 32.5 %), Panc-1 cells treated with **2b**
7 (apoptotic cells ~ 20.6 %).
8
9

10
11
12
13
14 Finally, the metabolic activity of Panc-1 cells treated with the designed compounds was
15 evaluated by a resazurin assay. Compound **2a** causes an inhibition of the metabolic activity
16 (IC_{50} = 0.26 μM) stronger than **2b** (IC_{50} = 0.9 μM) (Fig. 10 C). Moreover, **2a** caused a strong
17 inhibition (~ 80 %) of colony formation in two pancreatic cancer cells: Panc-1 and BxPC-3
18 (Supp. data, S7).
19
20
21
22
23
24
25

26 27 CONCLUSION

28
29 By setting up a streptavidin-biotin pull-down assay, we have demonstrated that **2a**, an
30 anthrafurandione with aminoethylamino side chains, which efficiently internalizes and
31 accumulates in the cytoplasm of Panc-1 cancer cells, targets *KRAS* mRNA under low-
32 abundance cellular conditions. Luciferase assays with specific vectors showed that **2a** and
33 its anthrathiophenedione analogue **2b** repress translation in a dose-response manner,
34 suggesting that they have a great potential in cancer therapy. Indeed, western blots showed
35 that these molecules strongly decrease the *KRAS* protein in Panc-1 cancer cells. Moreover,
36 the compounds activate apoptosis, as indicated by the caspase 3/7 and annexin/propidium
37 iodide assays, and reduce the metabolic activity as well as the colony formation of the cells.
38
39
40
41
42
43
44
45
46
47
48

49 The mechanism of action of the designed compounds **2a** and **2b** is based on their capacity
50 to bind to G4 structures located in the 5'-UTR of *KRAS* mRNA. The presence of these
51 folded structures in mRNA has been demonstrated by immunostaining in fixed cells.⁷⁶ A
52 recent study by Guo and Bartel casts doubts on the existence of RG4s under *in vivo*
53
54
55
56
57
58
59
60

1
2
3 conditions, as the authors found that RG4s are globally unfolded by single-stranded binding
4 proteins.⁷⁷ If this is also true for the *KRAS* transcripts in pancreatic cancer cells, compounds
5 **2a** and **2b** could inhibit translation by competing the binding of the single stranded-binding
6 proteins to the RNA G4-motifs.
7
8

9
10
11 Finally, having established in cancer cells that **2a** and **2b** have a potential as anticancer
12 agents, the next step will be *in vivo* testing. As pancreatic cancer cells are addicted to *KRAS*,
13 therapeutics targeting this oncogene should be much more injurious for the malignant cells
14 than for normal cells.
15
16
17
18
19
20
21

22 **EXPERIMENTAL**

23
24 **Oligonucleotides.** The oligonucleotides used in this study have been purchased from
25 Microsynth (Switzerland). Oligonucleotide solutions in DEPC-treated milliQ water have
26 been conserved at -80 °C. The sequences are reported in Table 1 and Supp. data, S8.
27
28
29
30
31
32
33

34 **Synthesis of 2a, 2b, 1a, 1b and biotinylated ligand b-2a**

35 **General information**

36
37
38
39 NMR spectra were recorded on a Varian VXR-400 instrument operated at 400 MHz
40 (¹H NMR) and 100 MHz (¹³C NMR). Chemical shifts were measured in DMSO-*d*₆ using
41 tetramethylsilane as an internal standard. Analytical TLC was performed using Silica Gel
42 F₂₅₄ plates (Merck) and column chromatography with a SilicaGel Merck 60. Melting points
43 were determined using a Buchi SMP-20 apparatus and are uncorrected. High-resolution
44 mass spectra were recorded with electron-spray ionization using a Bruker Daltonics
45 microOTOF-QII instrument. UV spectra were recorded on a Hitachi-U2000
46 spectrophotometer. HPLC was performed using a Shimadzu Class-VP V6.12SP1 system.
47
48
49
50
51
52
53
54
55
56 All solutions were dried over Na₂SO₄ and evaporated at reduced pressure using a Buchi-
57
58
59
60

R200 rotary evaporator at a temperature below 45 °C. All products were vacuum dried at room temperature. All solvents, chemicals and reagents were obtained commercially and used without purification. The ligands **2a**, **2b**, **1a** and **1b** have been synthesized as previously described.^{60,61} The purity of final conjugates **b-2a** was > 95 % as determined by HPLC analysis (Supp. data, S9).

Synthetic procedures

*tert-Butyl(6-(5-((3a*S*,4*S*,6a*R*)-2-oxohexahydro-1*H*-thieno[3,4-*d*]imidazol-4-yl)pentanamido)-hexyl) carbamate (2, *N*-Boc-HDA-Biotin)*

N-Boc-1,6-diaminohexane (0.50 g, 2.05 mmol) was added to a stirred solution of biotin (**1**, 0.50 g, 2.05 mmol), *N*-methylmorpholine (NMM, 0.23 mL, 2.05 mmol) and 1-[bis(dimethylamino)methylene]-1*H*-1,2,3-triazolo[4,5-*b*]pyridinium 3-oxid hexafluorophosphate (HATU, 0.77 g, 2.05 mmol) in dry DMF (20 mL). The reaction mixture was stirred overnight at room temperature, diluted with water and the product was extracted with ethyl acetate (2 × 25 mL). The extract was washed twice with water, dried and evaporated. The residue was purified by using column chromatography with chloroform-methanol (1:0□3:1) as the eluting solvent. The solid precipitate was recrystallized from *n*-propanol to give 0.84 g (89 %) of the white powder of *N*-Boc-HDA-Biotin (**2**);⁶³ mp 173-176 °C; ¹H NMR (400 MHz, DMSO-*d*₆) δ 7.73 (t, 1H, *J* = 5.4 Hz, NH); 6.77 (t, 1H, *J* = 5.0 Hz, NH); 6.43 (br s, 1H, NH-Biotin); 6.36 (br s, 1H, NH-Biotin); 4.31-4.28 (m, 1H, CH); 4.13-4.11 (m, 1H, CH); 3.11-3.06 (m, 1H, SCHCH₂); 3.01 (dd, 2H, *J*¹ = 6.2, *J*² = 7.8 Hz, NCH₂); 2.89 (dd, 1H, *J*¹ = 6.0, *J*² = 7.2 Hz, NCH₂); 2.81 (dd, 1H, *J*¹ = 5.2, *J*² = 7.5 Hz, SCHH); 2.57 (d, 1H, *J* = 12.4 Hz, SCHH); 2.03 (t, 2H, *J* = 7.5 Hz, COCH₂CH₂); 1.60-1.20 (m, 23H, C(CH₃)₃, 7CH₂); HRMS (ESI) calculated for C₂₁H₃₉N₄O₄S⁺ [M+H]⁺ 443.2687, found 443.2673.

1
2
3 *N*-(6-Aminohexyl)-5-((3*aS*,4*S*,6*aR*)-2-oxohexahydro-1*H*-thieno[3,4-*d*]imidazol-4-
4
5 *yl*)pentanamide trifluoroacetate (*HDA-Biotin*, **3**)
6

7 A solution of *N*-Boc-*HDA*-Biotin (**2**, 0.80 g, 1.81 mmol) in the mixture of DCM (10.0
8 ml) and TFA (2.0 ml) was stirred for 3 h at the room temperature. The solvent was
9 evaporated and residue re-precipitated from warm water with acetone. The precipitated
10 crystals were filtered, washed with acetone and dried to yield 0.72 g (87 %) of *HDA-Biotin*
11 (**3**); mp 92-95 °C; ¹H NMR (400 MHz, DMSO-*d*₆) δ 7.76 (t, 1H, *J* = 5.4 Hz, NH); 7.70 (br
12 s, 3H, NH₃); 6.42 (br s, 1H, NH-Biotin); 6.37 (br s, 1H, NH-Biotin); 4.32-4.29 (m, 1H,
13 CH); 4.14-4.11 (m, 1H, CH); 3.11-3.06 (m, 1H, SCHCH₂); 3.01 (dd, 2H, *J*¹ = 6.0, *J*² = 6.8
14 Hz, NCH₂); 2.82 (dd, 1H, *J*¹ = 5.0, *J*² = 7.5 Hz, SCHH); 2.76 (dd, 1H, *J*¹ = 6.0, *J*² = 7.2 Hz,
15 NCH₂); 2.58 (d, 1H, *J* = 12.6 Hz, SCHH); 2.04 (t, 2H, *J* = 7.5 Hz, COCH₂CH₂); 1.64-1.24
16 (m, 14H, 7CH₂); HRMS (ESI) calculated for C₁₆H₃₁N₄O₂S⁺ [M+H]⁺ 343.2162, found
17 343.2156.
18
19
20
21
22
23
24
25
26
27
28
29
30
31
32

33 *Biotinyl-N*-(6-aminohexyl)-4,11-dimethoxy-5,10-dioxo-5,10-dihydroanthra[2,3-*b*]furan-2-
34 *carboxamide* (**5**)
35
36

37 A mixture of 4,11-dimethoxyanthra[2,3-*b*]furan-5,10-dione-2-carboxylic acid (**4**⁶⁶;
38 0.30 g, 0.85 mmol), ethyldiisopropylamine (DIPEA, 0.5 ml, 3.00 mmol), biotinyl-*N*-(6-
39 aminohexyl)amine trifluoroacetate (**3**, 0.39 g, 0.85 mmol) and benzotriazol-1-yl-
40 oxytripyrrolidinophosphonium hexafluorophosphate (PyBOP, 0.52 g, 1.00 mmol) in DMSO
41 (15 ml) was stirred at room temperature for 1 h. The reaction mixture was diluted with
42 water and the product was extracted with ethyl acetate (2 × 20 mL). The extract was washed
43 twice with water, dried and evaporated. The residue was purified by using column
44 chromatography with chloroform-methanol (1:0-3:1) as the eluting solvent. The yield of
45 the orange solid of **5** was 0.46 g (80 %); mp 132-134 °C; ¹H NMR (400 MHz, DMSO-*d*₆) δ
46
47
48
49
50
51
52
53
54
55
56
57
58
59
60

1
2
3 8.87 (t, 1H, $J = 5.9$ Hz, NH); 8.05–8.03 (m, 2H, 6,9-H); 7.88 (s, 1H, 3-H); 7.82–7.80 (m,
4 2H, 7,8-H); 7.76 (t, 1H, $J = 5.3$ Hz, NH); 6.44 (br s, 1H, NH-Biotin); 6.37 (br s, 1H, NH-
5 Biotin); 4.31-4.27 (m, 1H, CH); 4.12 (s, 3H, OMe); 4.07 (s, 3H, OMe); 4.13-4.12-4.10 (m,
6 1H, CH); 3.28 (dd, 2H, $J^1 = 6.2$, $J^2 = 6.8$ Hz, NCH₂); 3.10-3.06 (m, 1H, SCHCH₂); 3.02
7 (dd, 2H, $J^1 = 6.0$, $J^2 = 7.0$ Hz, NCH₂); 2.81 (dd, 1H, $J^1 = 4.9$, $J^2 = 7.5$ Hz, SCHH); 2.56 (d,
8 1H, $J = 12.3$ Hz, SCHH); 2.04 (t, 2H, $J = 7.1$ Hz, COCH₂CH₂); 1.59-1.25 (m, 14H, 7CH₂);
9 ¹³C NMR (100 MHz, DMSO-*d*₆) δ 182.05 (C=O); 181.65 (C=O); 171.87 (N-C=O); 162.75
10 (N-CO-N); 156.92 (N-C=O); 151.61 (C); 150.47 (2C); 142.60 (C); 133.99 (C); 133.80 (C);
11 133.64 (C); 127.30 (C); 123.33 (C); 120.43 (C); 133.98 (CH); 126.10 (CH); 126.00 (CH);
12 108.44 (CH); 61.81 (CH); 61.71 (CH); 61.07 (OCH₃); 59.22 (OCH₃); 55.47 (CH); 39.86
13 (CH₂); 38.95 (CH₂); 38.31 (CH₂); 35.25 (CH₂); 29.15 (CH₂); 29.00 (CH₂); 28.24 (CH₂);
14 28.06 (CH₂); 26.19 (CH₂); 26.14 (CH₂); 25.38 (CH₂). HRMS (ESI) calculated for
15 C₃₅H₄₁N₄O₈S⁺ [M+H]⁺ 677.2640, found 677.2612.
16
17
18
19
20
21
22
23
24
25
26
27
28
29
30
31
32

33 *4,11-bis((2-Aminoethyl)amino)-biotinyl-N-(6-aminohexyl)-5,10-dioxo-5,10-*
34 *dihydroanthra[2,3-b]furan-2-carboxamide (6, b-2a)*
35

36
37 A mixture of compound **5** (0.27 g, 0.40 mmol) and ethylenediamine (1.5 mL) in THF
38 (5.0 mL) was heated at 50 °C for 2-3 h. During this time, the yellow color of the reaction
39 mixture changed to dark blue, and after the complete conversion of **5** (as determined by
40 TLC) the solution was cooled and quenched with water. An aqueous solution of HCl (1%)
41 was added to make the pH=8.0, the solution was saturated with NaCl, and the product was
42 extracted with warm *n*-butanol (3 × 25 mL). The extract was washed twice with brine, dried
43 and evaporated. The residue was purified by column chromatography using chloroform-
44 methanol-concentrated NH₄OH (10:2:0□10:4:1) as the eluting solvent. The purified residue
45 was dissolved in a warm aqueous solution of HCl (1N) and re-precipitated with acetone.
46
47
48
49
50
51
52
53
54
55
56
57
58
59
60

The precipitated crystals were filtered, washed with acetone and dried to yield 0.22 g (68%) of the dark blue powder of dihydrochloride **6**; mp 204-206 °C (decomp.); HPLC Kromasil-100-5- μ m C-18 column (4 \times 250 mm, LW = 260 nm), eluent: A – H₃PO₄ (0.01 M), B – MeCN; gradient B 20–60% (30 min), elution time 9.4 min, purity 96 %. ¹H NMR (400MHz, DMSO-*d*₆) δ 12.18 (t, 1H, *J* = 5.0 Hz, NH); 11.36 (t, 1H, *J* = 5.5 Hz, NH); 9.32 (t, 1H, *J* = 5.4 Hz, NH); 8.55 (s, 1H,3-H); 8.41 (br s, 3H, NH₃); 8.25–8.22 (m, 2H, 6,9-H); 8.18 (br s, 3H, NH₃); 7.82 (br s, 1H, NH); 7.80–7.78 (m, 2H, 7,8-H); 6.44 (br s, 1H, NH-Biotin); 6.39 (br s, 1H, NH-Biotin); 4.31-4.28 (m, 1H, CH); 4.13-4.10 (m, 3H, CH, NCH₂); 4.08-4.06 (m, 2H, 2NCH₂); 3.29-3.26 (m, 4H, 2NCH₂); 3.10-3.06 (m, 1H, SCHCH₂); 3.05-3.00 (m, 2H, NCH₂); 2.81 (dd, 1H, *J*¹ = 5.1, *J*² = 7.3 Hz, SCHH); 2.57 (d, 1H, *J* = 12.4 Hz, SCHH); 2.05 (t, 2H, *J* = 7.3 Hz, COCH₂CH₂); 1.60-1.30 (m, 14H, 7CH₂). HRMS (ESI) calculated for C₃₇H₄₉N₈O₆S⁺ [M+H]⁺ 733.3490, found 733.3494.

Cell culture, metabolic activity and proliferation assays

Panc-1 and BxPC-3 cells (Human pancreatic cancer cells) were maintained in exponential growth in Dulbecco's Modified Eagle's Medium (DMEM) containing 100 U/mL penicillin, 100 mg/mL streptomycin, 20 mM L-glutamine and 10 % fetal bovine serum (Euroclone, Italy). The cell lines have been genotyped by Microsynth (Switzerland) to verify their identity. They matched 100 % with the DNA-profiles of Panc-1 (ATCC[®] CRL-1469TM) and BxPC-3 (ATCC[®] CRL-1687TM). The metabolic activity assay was performed by seeding the cells (10 x 10³ cells/well) in a 96-well plate. After one day the cells have been treated with the compounds and after an incubation of 72 hours the resazurin assay was performed following a standard procedure.

Colony forming assays have been carried out with Panc-1 and BxPC-3 cells plated in a 60-mm plate and treated with 0.25 and 0.5 μ M **2a** or 1 and 1.5 μ M **2b**. After 18 days, the cells

1
2
3 were fixed and stained for 10 min with 2.5 % methylene blue in 50 % ethanol. Colonies
4
5 with > 50 cells were counted.
6
7
8
9

10 **Circular dichroism spectra and UV-melting curves**

11
12
13 CD spectra have been obtained on a JASCO J-600 spectropolarimeter, equipped with a
14 thermostated cell holder, with 5 μ M oligonucleotide solutions in 50 mM Na-cacodylate pH
15 7.4, 100 mM KCl or LiCl (RNase free). The CD spectra (for *KRAS utr-1*, *utr-c* and *utr-z*)
16 and *NRAS* were registered at 25 and 90 °C. Spectra were recorded in 0.5 cm quartz cuvette.
17
18 The spectra were calculated with J-700 Standard Analysis software (Japan Spectroscopic
19 Co, Ltd). Each spectrum was recorded three times, smoothed and the baseline subtracted.
20
21 UV melting curves were obtained by using JASCO V-750 UV-visible spectrophotometer
22 equipped with a temperature control system that heat/cool the sample through a Peltier
23 technology (ETCS-761) (Jasco, USA). Melting curves were recorded at 260 and 296 nm in
24 a 0.5 cm path length quartz cuvette heating the sample from 20 to 100 °C. The samples
25 were prepared at a final concentration of 5 μ M in 100 mM KCl and 50 mM Na-cacodylate,
26 pH 7.4. Incubation with increasing amount of the molecules (**2a** and **2b**) ($r=1, 2$ and 4) was
27 performed for 1 h at room temperature.
28
29
30
31
32
33
34
35
36
37
38
39
40
41
42
43
44

45 **RNase T1 footprinting and electrophoretic mobility-shift assay**

46
47 Single-stranded RNAs were purified by PAGE and 5'-end labeled with T4
48 polynucleotide kinase (ThermoFisher, USA) and [³²P]-ATP (Perkin Elmer, USA) for 1.5 h
49 at 37 °C. RNase T1 footprinting were performed with 30 nM s-80 heated for 5 min at 85°C
50 and then incubated overnight at 25 °C in 10x Structure Buffer (RNase T1 Biochemistry
51
52
53
54
55
56
57
58
59
60

1
2
3 Grade, ThermoFisher, USA) with 100 mM KCl or LiCl. The reactions were performed with
4
5 0.05 units of RNase T1 (ThermoFisher, USA) for 10 min at 25 °C and stopped with 20 µl
6
7 inactivation/precipitation buffer (ThermoFischer, USA). RNA was let to precipitate at -80
8
9 °C for 2 h and centrifuged for 30 min at 13000 rpm. Precipitated RNA was resuspended
10
11 with loading buffer (ThermoFisher, USA), heated for 5 min at 95 °C and electrophoresed
12
13 on a 20 % denaturing gel, pre-equilibrated at 55 °C in a Sequi-Gen GT Nucleic Acids
14
15 Electrophoresis Apparatus (Bio-Rad, USA), equipped with a thermocouple that allows a
16
17 precise temperature control. EMSA assays were performed with 20 nM *utr-z* or *s-80* labeled
18
19 at the 5'-end with [³²P]-ATP. The mixture was incubated for 30 min at 37 °C with
20
21 increasing concentrations of antibody BG4 (1 and 2 µg). BG4 was produced according to
22
23 Studier et al.⁷⁸ The samples were run in a 5 % TBE 1x gel for 2 h. After running, the gel
24
25 was fixed in a solution containing 10 % acetic acid and 10 % methanol, dried at 80 °C and
26
27 exposed to Hyperfilm MP (GE Healthcare) for autoradiography.
28
29
30
31
32
33

34 **Western blots**

35
36
37 Total protein lysates (15 µg) were electrophoresed on 12 % SDS-PAGE and transferred
38
39 to a nitrocellulose membrane at 70 V for 2 h. The filter was blocked for 1 h with 5 % BSA
40
41 solution in PBS 0.05 % Tween (Sigma-Aldrich, USA) at room temperature. The primary
42
43 antibodies used are anti-actin (clone JLA20, IgM mouse, 1x10⁻⁴ µg/mL, Calbiochem,
44
45 Merck Millipore, Germany), anti-KRAS (IgG rabbit polyclonal antibody, diluted 1:250, ab
46
47 102007, Abcam, United Kingdom). Membranes with the samples were incubated overnight
48
49 at 4 °C with primary antibodies. The filters were washed with a 0.05 % Tween in PBS and
50
51 subsequently incubated for 1 h with the secondary antibodies horseradish peroxidase
52
53 conjugated: anti-mouse IgM (diluted 1:2000) and anti-rabbit IgG (diluted 1:5000)
54
55
56
57
58
59
60

1
2
3 (Calbiochem, Merck Millipore, Germany). The signal of the proteins was developed with
4 Super Signal ®West PICO, and FEMTO (Thermo Fisher, USA) and detected with
5 ChemiDOC XRS, Quantity One 4.6.5 software (BioRad Laboratories, USA).
6
7
8
9

10 11 12 13 **RNA extraction and quantitative real-time PCR**

14
15 Panc-1 cells were plated in a 96-well plate (18×10^3 cells/well). The following day (24
16 h), we treated the cells with **2a**, **2b**, **1a** and **1b** and total RNA was extracted by using iScript
17™ RT-qPCR Sample Preparation Reagent (BioRad, USA) 6 and 24 hours after treatment,
18 following the manufacturer's instructions. For the cDNA synthesis, 1.25 µl of RNA was
19 heated at 70 °C and placed on ice. The solution was added with 11.5 µl of a mix containing:
20 1x buffer, 0.01 M DTT (Invitrogen, USA), 1.6 µM primer dT [MWG Biotech, Germany;
21 d(T)₁₆], 1.6 µM random hexamer primers (Mycrosynth, Switzerland), 0.4 mM dNTPs
22 solution containing equimolar amounts of dATP, dCTP, dGTP and dTTP (Euroclone, Italy),
23 0.8 U/µl RNase OUT, 8 U/µl of M-MLV reverse transcriptase (Invitrogen, USA). The
24 mixtures were incubated for 1 h at 37 °C and stopped by heating at 95 °C for 5 min. As a
25 negative control the reverse transcription reaction was performed with a sample containing
26 DEPC-treated water.
27
28
29
30
31
32
33
34
35
36
37
38
39
40

41 To determine the levels of *KRAS* and housekeeping genes hypoxanthine-guanine
42 phosphoribosyltransferase (HPRT) and β2-microglobulin, quantitative real-time multiplex
43 reactions were performed. We used 1 x Kapa Probe fast qPCR kit (KAPA Biosystems,
44 USA), 2.2 µl of cDNA and primers/probes (sequences are reported in Supp. data, S8). The
45 PCR cycle was: 3 min at 95 °C, 50 cycles 10 s at 95 °C, 60 s at 58 °C. PCR reactions were
46 carried out with a CFX-96 real-time PCR apparatus controlled by an Optical System
47 software (version 3.1) (Bio-Rad Laboratories, USA). The *KRAS* transcript level was
48 normalized with the housekeeping genes.
49
50
51
52
53
54
55
56
57
58
59
60

Dual luciferase assays

Panc-1 cell were plated (20×10^3) and the following day treated with increasing concentrations of compounds **2a**, **2b**, **1a** and **1b** (0.3-1.6 μ M). After 6 h of treatment, the cells were transfected with the plasmids. The 192 nt of *KRAS* 5'UTR (NM_033360) was cloned between Hind III and Nhe I of pRL-CMV plasmid (GenScript, USA). Transfection was performed by mixing vectors (10 ng/well) p-light-SwitchGear *KRAS* (SwitchGear Genomics,USA) (in the text pRL-*KRAS*) or pRL-CMV-UTR or pRL-CMV (*Renilla luciferase*) with 200 ng of control plasmid (pHRAS-mutA-luc) (*Firefly luciferase*) using jet-PEI (Polyplus, France) as transfectant agent. *Renilla luciferase* in cell lysates was measured and normalized by *Firefly luciferase*. Luciferase assays were performed 48 h after transfection with Dual-Glo Luciferase Assay System (Promega, USA) following the supplier instructions. Samples were read on a Turner Luminometer and the relative luminescence expressed as (T/C x 100) where T= *Renilla luciferase*/*Firefly luciferase* in treated cells and C= *Renilla luciferase* / *Firefly luciferase* in untreated cells.

Uptake analysis

Panc-1 cells were plated in a 24-well plate at density of 5×10^4 cells/well. After one day, the cells were treated with the molecules: time and concentration as indicated in figure captions. The cells were trypsinized and pelleted. The pellets were resuspended in 200 μ l PBS and immediately analyzed by FACScan Flow Cytometer (Becton Dickinson, USA) equipped with a 488 nm argon laser. A minimum of 10^4 cells for each sample were acquired in list mode and analyzed using Cell Quest software. The cell population was analyzed by FSC light and SSC light. The signal was detected by FL3 (680 nm) channel in log scale.

Apoptosis assays

Caspase activity assay was performed with Apo-ONE™ Homogeneous Caspase-3/7 Assay (Promega, USA), according to the manufacturer's protocol. Annexin V–propidium iodide assay was performed with Annexin V Apoptosis Detection Kit (Santa Cruz, USA), following the manufacturer's instructions. Flow cytometry measurements were performed with FACScan Flow Cytometer (Becton Dickinson, USA).

Biotin-streptavidin pull-down experiments

Calibration plot. To construct the calibration plot for biotin-streptavidin pull down assays, we prepared several mixtures of 115- and 89-nt sequences in 50 mM Tris-HCl, pH 7.4, 100 mM KCl at total concentration of 0.2 μ M and 115-nt/89-nt ratio varying from 1 to 5000. The mixtures have been amplified with KAPA2G Robust HotStart PCR Kit (KAPA Biosystems, USA) using the same couple of primers (sequences reported in Supp. data, S8) (0.5 μ M) and dNTPs (0.2 mM). The program was: 5 min 95 °C, 15 sec 95 °C, 15 sec 55 °C, 30 sec 72 °C, 35 cycles. The products have been separated by 8% PAGE and the bands stained with ethidium bromide. Their intensities were measured with a ChemiDOC XRS, Quantity One 4.6.5 software (BioRad Laboratories, USA). We reported in a plot the ratio of the intensities of the amplified bands (115-nt/89-nt) as a function of the logarithm of the ratio (r) of the two sequences in the mixtures. We obtained a straight line that correlated the band intensities with the mixture composition.

Pull-down with cellular RNA. Total RNA was extracted from Panc-1 cells and its concentration was measured by UV absorption. 8 μ g of cellular RNA in 50 mM KCl, 50 mM Tris-HCl, pH 7.4 was incubated overnight with increasing concentrations of **b-2a** (from 0.4 to 0.8 μ M). We incubated the magnetic beads, after saturation with ssDNA (vide infra) with cellular RNA treated with the biotinylated ligand for 20 min at 25 °C. The supernatant

was removed and the beads washed twice with Tris buffer. We then recovered the bound RNA with a solution 0.8 M NaCl. The recovered RNA was retro-transcribed with 0.8 U/ μ l RNase OUT; 8 U/ μ l of M-MLV reverse transcriptase (Life Technologies, Thermo Fisher, USA) and amplified by quantitative real-time PCR (vide infra). We amplified *KRAS* and the housekeeping genes HPRT and β 2-microglobulin (for primers see Supp. data, S8).

Table 1. G4 motifs in s-80, the first 80 nt in the *KRAS* 5'-UTR mRNA.

	Position	Sequence (5'→3')	G/C ^(a)	G-score	T_M ^(b)	G4-RNA ΔG ^(c) (kcal/mol)
<i>utr-1</i>	16-30	GCGGC GG C GG C GG AGGCA	4	21	53	-4.9
<i>utr-z</i>	36-55	GG C GG C GG CAGU GG C GG C GG	2.6	21	64	-3.7
<i>utr-c</i>	59-71	AGGUG GG C GG C GG C	4	21	52	-5.6

^(a) G/C ratio of the G4 motifs (>1.5 favors G4 over loop-hairpin);³⁷

^(b) T_M obtained in 50 mM Na-cacodylate, pH 7.4, 100 mM KCl;

^(c) ΔG s (298 K) obtained from UV-melting curves, using a two-state model.

Table 2. K_D values relative to the interaction between *KRAS* G4 RNAs and ligands **2a** and **2b**.

	Sequence (5'→3')	2a K_D (nM) ^(a)	2b K_D (nM) ^(a)
<i>utr-1</i>	GCGGC GG C GG C GG AGGCA	75 ± 6	91 ± 15

<i>utr-z</i>	GGCGGCGGCAGUGGCGGCGG	251 ± 151	294 ± 138
<i>utr-4</i> ^(b)	CAGCAGC GGCGGCGGCAGUGG	96 ± 45	83 ± 27
<i>WC hairpin</i> ^(c)	CCGCCGCAGUGGCGGCGG	514 ± 103	482 ± 109

^(a) obtained from fluorescence titrations in 50 mM Tris-HCl, pH 7.4, 100 mM KCl;

^(b) G4 motif present in the *KRAS* 5'UTR that overlaps other G4 motifs;

^(c) W.C. RNA hairpin with 7-C:G stem and 4-nt loop (AGUG) .

ASSOCIATED CONTENT

Supplementary data: Scheme illustrating how RG4 can regulate translation initiation; Thermal difference spectra of RG4s; *KRAS* 5'-UTR sequences in mammals; Fluorescence titrations; UV and NMR spectra, HPLC-chromatograms; confocal microscopy; colony forming assay; DNA and RNA sequences used in the study. This material is available free of charge via the Internet at <http://pubs.acs.org>.”

AUTHOR INFORMATION

Corresponding Author

* Luigi E. Xodo, Department of Medical and Biological Sciences, University of Udine, P.le Kolbe 4, 33100 Udine, Italy, Tel. +39.0432.494395; Fax +39.0432.494301, E-mail.

luigi.xodo@uniud.it

Author Contributions

This study was conceived and written by LEX and GM. AST and AS have designed and synthesized the G4 ligands, GM and SC have performed the experiments. JM and GC have prepared and purified BG4. All authors have given approval to the final version of the manuscript.

Funding Sources

This work has been carried out with the financial support of AIRC (Italian association for cancer research). IG2013, project Code 143

ABBREVIATIONS

KRAS, Kirsten ras gene; PDAC, pancreatic ductal adenocarcinoma cells; RG4, RNA G-quadruplex; Panc-1, pancreatic cancer cells; BxPC-3, pancreatic cancer cells; ATPD, antrathiophenediones; 5'-UTR, 5'-untranslated region; ATFD, antrafurandiones; DCM, dichloromethane; HATU, 1-[bis(dimethylamino)methylene]-1*H*-1,2,3-triazolo[4,5-*b*]pyridinium 3-oxid hexafluorophosphate; NMM, *N*-methyilmorpholine; PyBOP, benzotriazol-1-yl-oxytripyrrolidinophosphonium hexafluorophosphate; DIPEA, ethyldiisopropylamine; THF, tetrahydrofuran; TFA, trifluoroacetic acid; ThT, thioflavin T.

REFERENCES

1. Vigil, D.; Cherfils, J.; Rossman, K.L.; Der, C.J. Ras superfamily GEFs and GAPs: validated and tractable targets for cancer therapy? *Nat. Rev. Cancer* **2010**, *10*, 842-857.
2. Rodriguez-Viciana, P.; Sabatier, C.; McCormick, F. Signaling specificity by Ras family GTPases is determined by the full spectrum of effectors they regulate. *Mol. Cell Biol.* **2004**, *24*, 4943-4945.
3. Wortzel, I.; Seger, R. The ERK cascade: distinct functions within various subcellular organelles. *Genes Cancer* **2011**, *2*, 195-209.
4. Castellano, E.; Downward, J. Ras interaction with PI3K: more than just another effector pathway. *Genes Cancer* **2011**, *2*, 261-274.

- 1
2
3 5. Schubbert, S.; Shannon, K.; Bollag, G. Hyperactive Ras in developmental disorders and
4
5 cancer. *Nat. Rev. Cancer* **2007**, *7*, 295-308.
6
- 7 6. Ryan, D.P.; Hong, T.S.; Bardeesy, N. Pancreatic adenocarcinoma. *N. Engl. J. Med.*
8
9 **2014**, *371*, 2140-2141.
10
- 11 7. Prior, I.A.; Lewis, P.D.; Mattos, C. A comprehensive survey of Ras mutations in cancer.
12
13 *Cancer Res.* **2012**, *72*, 2457-2467.
14
- 15 8. Karnoub, A.E.; Weinberg, R.A. Ras oncogenes: split personalities. *Nat. Rev. Mol. Cell*
16
17 *Biol.* **2008**, *9*, 517-531.
18
- 19 9. Collins, M.A.; Bednar, F.; Zhang, Y.; Brisset, J.C.; Galbán, S.; Galbán, C.J.; Rakshit,
20
21 S.; Flannagan, K.S.; Adsay, N.V.; Pasca di Magliano, M. Oncogenic Kras is required
22
23 for both the initiation and maintenance of pancreatic cancer in mice. *J. Clin. Invest.*
24
25 **2012**, *122*, 639-653.
26
- 27 10. Kanda, M.; Matthaei, H.; Wu, J.; Hong, S.M.; Yu, J.; Borges, M.; Hruban, R.H.; Maitra,
28
29 A.; Kinzler, K.; Vogelstein, B.; Goggins, M. Presence of somatic mutations in most
30
31 early-stage pancreatic intraepithelial neoplasia. *Gastroenterology* **2012**, *142*, 730-733.
32
33
- 34 11. Vincent, A.; Herman, J.; Schulick, R.; Hruban, R.H.; Goggins, M. Pancreatic cancer.
35
36 *Lancet* **2011**, *378*, 607-620.
37
- 38 12. Ying, H.; Kimmelman, A.C.; Lyssiotis, C.A.; Hua, S.; Chu, G.C.; Fletcher-Sananikone,
39
40 E.; Locasale, J.W.; Son, J.; Zhang, H.; Coloff, J.L.; Yan, H.; Wang, W.; Chen, S.; Viale,
41
42 A.; Zheng, H.; Paik, J.H.; Lim, C.; Guimaraes, A.R.; Martin, E.S.; Chang, J.; Hezel,
43
44 A.F.; Perry, S.R.; Hu, J.; Gan, B.; Xiao, Y.; Asara, J.M.; Weissleder, R.; Wang, Y.A.;
45
46 Chin, L.; Cantley, L.C.; DePinho, R.A. Oncogenic Kras maintains pancreatic tumors
47
48 through regulation of anabolic glucose metabolism. *Cell* **2012**, *149*, 656-670.
49
- 50 13. Son, J.; Lyssiotis, C.A.; Ying, H.; Wang, X.; Hua, S.; Ligorio, M.; Perera, R.M.;
51
52
53 Ferrone, C.R.; Mullarky, E.; Shyh-Chang, N.; Kang, Y.; Fleming, J.B.; Bardeesy, N.;
54
55
56
57
58
59
60

- 1
2
3 Asara, J.M.; Haigis, M.C.; DePinho, R.A.; Cantley, L.C.; Kimmelman, A.C. Glutamine
4 supports pancreatic cancer growth through a KRAS-regulated metabolic pathway.
5
6 *Nature*, **2013** *496*, 101-105.
7
8
9 14. Weinstein, I.B.; Joe, A. Oncogene addiction. *Cancer Res.* **2008**, *68*, 3077-80.
10
11 15. Patricelli, M.P.; Janes, M.R.; Li, L.S.; Hansen, R.; Peters, U.; Kessler, L.V.; Chen, Y.;
12 Kucharski, J.M.; Feng, J.; Ely, T.; Chen, J.H.; Firdaus, S.J.; Babbar, A.; Ren, P.; Liu, Y.
13 Selective inhibition of oncogenic KRAS output with small molecules targeting the
14 inactive state *Cancer Discovery* **2016**, *6*, 316-329.
15
16 16. Wilson, C.Y.; Tolias, P. Recent advances in cancer drug discovery targeting RAS. *Drug*
17 *Discovery Today* **2016**, *21*, 1915-1919.
18
19 17. Stephen, A.G.; Esposito, D.; Bagni, R.K.; McCormick, F. Dragging ras back in the ring.
20 *Cancer Cell* **2014**, *25*, 272-281.
21
22 18. Ostrem, J.M.; Shokat, K.M. Direct small-molecule inhibitors of KRAS: from structural
23 insights to mechanism-based design. *Nat. Rev. Drug Discovery* **2016**, *15*, 771-785.
24
25 19. Kiessling, M.K.; Rogler, G. Targeting the ras pathway by mitogene-activated protein
26 kinase inhibitors. *Swiss Med. Wkly.* **2015**, *145*, w14207.
27
28 20. Li, T.; Sparano, J.A. Farnesyl transferase inhibitors. *Cancer Invest.* **2008**, *26*, 653-661.
29
30 21. Cox, A.D.; Der, C.J.; Philips, M.R. Targeting RAS membrane association: back to the
31 future for anti-RAS drug discovery. *Clin. Cancer Res.* **2015**, *21*, 1819-1827.
32
33 22. Tamanoi, F.; Lu, J. Recent progress in developing small molecule inhibitors designed to
34 interfere with ras membrane association: toward inhibiting KRAS and NRAS functions.
35 *Enzymes* **2013**, *34*, Pt. B:181-200.
36
37 23. Cogoi, S.; Paramasivam, M.; Spolaore, B.; Xodo, L.E. Structural polymorphism within
38 a regulatory element of the human KRAS promoter: formation of G4-DNA recognized
39 by nuclear proteins. *Nucleic Acids Res.* **2008**, *36*, 3765-3780.
40
41
42
43
44
45
46
47
48
49
50
51
52
53
54
55
56
57
58
59
60

- 1
2
3 24. Faudale, M.; Cogoi, S.; Xodo, L.E. Photoactivated cationic alkyl-substituted porphyrin
4 binding to g4-RNA in the 5'-UTR of KRAS oncogene represses translation. *Chem.*
5 *Commun. (Camb)* **2012**, *48*, 874-876.
6
7
8
9 25. Rapozzi, V.; Zorzet, S.; Zacchigna, M.; Della Pietra, E.; Cogoi, S.; Xodo, L.E.
10 Anticancer activity of cationic porphyrins in melanoma tumour-bearing mice and
11 mechanistic in vitro studies. *Mol. Cancer* **2014**, *13*, 75-92.
12
13
14
15 26. Kumari, S.; Bugaut, A.; Huppert, J.L.; Balasubramanian, S. An RNA G-quadruplex in
16 the 5'-UTR of the NRAS proto-oncogene modulates translation. *Nat. Chem. Biol.* **2007**,
17 *3*, 218-221.
18
19
20
21 27. Bugaut, A.; Balasubramanian, S. 5'-UTR RNA G-quadruplexes: translation regulation
22 and targeting. *Nucl. Acids Res.* **2012**, *40*, 4727-4741.
23
24
25
26 28. Siddiqui-Jain, A.; Grand, C.L.; Bearss, D.J.; Hurley, L.H. Direct evidence for a G-
27 quadruplex in a promoter region and its targeting with a small molecule to repress c-
28 MYC transcription. *Proc. Natl. Acad. Sci. U. S. A.* **2002**, *99*, 11593-11598.
29
30
31
32 29. Bochman, M.L.; Paeschke, K.; Zakian, V.A. DNA secondary structures: stability and
33 function of G-quadruplex structures. *Nat. Rev. Genet.* **2012**, *13*, 770-780.
34
35
36
37 30. Murat, P.; Balasubramanian, S. Existence and consequences of G-quadruplex structures
38 in DNA. *Curr. Opin. Gen. Dev.* **2014**, *25*, 22-29.
39
40
41
42 31. Burge, S.; Parkinson, G.N.; Hazel, P.; Todd, A.K.; Neidle, S. Quadruplex DNA:
43 sequence, topology and structure. *Nucleic Acids Res.* **2006**, *34*, 5402-5415.
44
45
46 32. Balasubramanian, S.; Hurley, L.H.; Neidle, S. Targeting G-quadruplexes in gene
47 promoters: a novel anticancer strategy? *Nat. Rev. Drug Discovery* **2011**, *10*, 261-275.
48
49
50 33. Maizels, N. G4 motifs in human genes. *Ann. N. Y. Acad. Sci.* **2012**, *1267*, 53-60.
51
52
53 34. Mendoza, O.; Bourdoncle, A.; Boulé, J.B.; Brosh, R.M. Jr.; Mergny, J.L. G-
54 quadruplexes and helicases. *Nucleic Acids Res.* **2016**, *44*, 1989-2006.
55
56
57
58
59
60

- 1
2
3 35. Cogoi, S.; Xodo, L.E. G4 DNA in ras genes and its potential in cancer therapy.
4
5 *Biochim. Biophys. Acta.* **2016**, *1859*, 663-674.
6
7 36. Hänsel-Hertsch, R.; Beraldi, D.; Lensing, S.V.; Marsico, G.; Zyner, K.; Parry, A.; Di
8
9 Antonio, M.; Pike, J.; Kimura, H.; Narita, M.; Tannahill, D.; Balasubramanian, S. G-
10
11 quadruplex structures mark human regulatory chromatin. *Nat. Genet.* **2016**, *48*, 1267-
12
13 1272.
14
15 37. Beaudoin, J.D.; Perreault, J.P. 5'-UTR G-quadruplex structures acting as translational
16
17 repressors. *Nucleic Acids Res.* **2010**, *38*, 7022-7036.
18
19 38. Jodoin, R.; Nauer, L.; Garant, J.M.; Mahdi Laaref, A.; Phaneuf, F.; Perreault, J.P. The
20
21 folding of 5'-UTR human G-quadruplexes possessing long central loop. *RNA* **2014**,
22
23 *20*, 1129-1141.
24
25 39. Hinnebusch, A.G.; Ivanov, I.P.; Sonenberg, N. Translational control by 5'-
26
27 untranslated regions of eukaryotic mRNAs. *Science* **2016**, *352*, 1413-1416.
28
29 40. Song, J.; Perreault, J.P.; Topisirovic, I.; Richard, S. RNA G-quadruplexes and their
30
31 potential regulatory roles in translation. *Translation* **2016**, *4*, e1244031.
32
33 41. Gomez, D.; Guédin, A.; Mergny, J.L.; Salles, B.; Riou, J.F.; Teulade-Fichou, M.P.;
34
35 Calsou, P. A G-quadruplex structure within the 5'-UTR of TRF2 mRNA represses
36
37 translation in human cells. *Nucleic Acids Res.* **2010**, *38*, 7187-7198.
38
39 42. Kwok, C.K.; Ding, Y.; Shahid, S.; Assmann, S.M.; Bevilacqua, P.C. A stable RNA G-
40
41 quadruplex within the 5'-UTR of Arabidopsis thaliana ATR mRNA inhibits
42
43 translation. *Biochem. J.* **2015**, *467*, 91-102.
44
45 43. Arora, A.; Dutkiewicz, M.; Scaria, V.; Hariharan, M.; Maiti, S.; Kurreck, J. Inhibition
46
47 of translation in eukaryotic cells by an RNA G-quadruplex motif. *RNA* **2008**, *14*, 1290-
48
49 1296.
50
51
52
53
54
55
56
57
58
59
60

- 1
2
3 44. Kumari, S.; Bugaut, A.; Balasubramanian, S. Position and stability are determining
4
5 factors for translation repression by an RNA G-quadruplex forming sequence within
6
7 5'-UTR of the NRAS proto oncogene. *Biochemistry* **2008**, *47*, 12664-12669.
8
9
10 45. Morris, M.J.; Negishi, Y.; Pazsint, C.; Schonhoft, J.D.; Basu, S. A RNA G-quadruplex
11
12 is essential for cap-independent translation initiation in human VEGF IRES. *J. Am.*
13
14 *Chem. Soc* **2010**, *132*, 17831-17839.
15
16 46. Lammich, S.; Kamp, F.; Wagner, J.; Nuscher, B.; Zilow, S.; Ludwig, A.K.; Willem,
17
18 M.; Haass, C. Translational repression of the disintegrin and metallo protease
19
20 ADAM10 by a stable G-quadruplex secondary structure in its 5'-untranslated region.
21
22 *J. Biol. Chem.* **2011**, *286*, 45063-45072.
23
24 47. Bolduc, F.; Garant, J.M.; Allard, F.; Perreault, J.P. Irregular G-quadruplexes found in
25
26 untranslated regions of human mRNAs influences translation. *J. Biol. Chem.* **2016**,
27
28 *291*, 21751-21750.
29
30
31 48. Zucker, M. Mfold web server for nucleic acid folding and hybridization prediction
32
33 *Nucleic Acids Res.* **2003**, *31*, 3406-3415.
34
35 49. Kikin, O.; D'Antonio, L.; Bagga, P.S. QGRS Mapper: a web-based server for
36
37 predicting G-quadruplexes in nucleotide sequences. *Nucleic Acids Res.* **2006**, *34*,
38
39 W676–W682.
40
41
42 50. Vorlickova, M.; Kejnovska, I.; Bednarova, K.; Renciuk, D.; Kypr, J. Circular
43
44 dichroism spectroscopy of DNA: from duplexes to quadruplexes. *Chirality* **2012**, *24*,
45
46 691-698.
47
48 51. Mergny, J.L.; Li, J.; Lacroix, L.; Amrane, S.; Chaires, J.B. Thermal difference spectra: a
49
50 specific signature for nucleic acid structures. *Nucleic Acids Res.* **2005**, *33*, e138.
51
52
53 52. Yangyuoru, P.M.; Di Antonio, M.; Ghimire, C.; Biffi, G.; Balasubramanian, S.; Mao, H.
54
55 Dual binding of an antibody and a small molecule increases the stability of TERRA G-
56
57
58
59
60

- 1
2
3 quadruplex. *Angew. Chem. Int. Ed. Engl.* **2015**, *54*, 910-913.
4
5 53. Biffi, G.; Tannahill, D.; McCafferty, J.; Balasubramanian, S. Quantitative
6
7 visualization of DNA G-quadruplex structures in human cells. *Nat. Chem.* **2013**, *5*,
8
9 182-186.
10
11 54. Miserachs, H.G.; Donghi, D.; Borner, R.; Johannsen, S.; Sigel, R.K.O. Distinct
12
13 differences in metal ion specificity of RNA and DNA G-quadruplexes. *J. Biol. Inorg.*
14
15 *Chem.* **2016**, *21*, 975-986.
16
17 55. McPike, M.P.; Goodisman, J.; Dabrowiak, J.C. Drug-RNA footprinting. *Methods*
18
19 *Enzymol.* **2001**, *340*, 431-449.
20
21 56. Xu, S.; Li, Q.; Xiang, J.; Yang, Q.; Sun, H.; Guan, A.; Wang, L.; Liu, Y.; Yu, L.; Shi,
22
23 Y., Chen, H.; Tang, Y. Thioflavin T as an efficient fluorescence sensor for selective
24
25 recognition of RNA G-quadruplexes. *Sci. Rep.* **2016**, *6*, 24793.
26
27 57. Weldon, C.; Behm-Ansmant, I.; Hurley, L.H.; Burley, G.A.; Branlant, C.; Eperon,
28
29 I.C.; Dominguez, C. Identification of G-quadruplexes in long functional RNAs using
30
31 7-deazaguanine RNA. *Nat. Chem. Biol.* **2017**, *13*, 18-20.
32
33 58. Bugaut, A.; Rodriguez, R.; Kumari, S.; Hsu, S.T.; Balasubramanian, S.
34
35 Small molecule-mediated inhibition of translation by targeting a native RNA G-
36
37 quadruplex. *Org. Biomol. Chem.* **2010**, *8*, 2771-2776
38
39 59. Katsuda, Y.; Sato, S.; Asano, L.; Morimura, Y.; Furuta, T.; Sugiyama, H.; Hagihara,
40
41 M.; Uesugi, M. A small molecule that represses translation of G-quadruplex-containing
42
43 mRNA. *J. Am. Chem. Soc.* **2016**, *138*, 9037-9040.
44
45 60. Cogoi, S.; Shchekotikhin, A.E.; Membrino, A.; Sinkevich, Y.B.; Xodo, L.E.
46
47 Guanidino anthrathiophenediones as G-quadruplex binders: uptake, intracellular
48
49 localization, and anti-Harvey-Ras gene activity in bladder cancer cells. *J. Med. Chem.*
50
51 **2013**, *56*, 2764-2778.
52
53
54
55
56
57
58
59
60

- 1
2
3 61. Cogoi, S.; Zorzet, S.; Shchekotikhin, A.E.; Xodo, L.E. Potent apoptotic response
4 induced by chloroacetamide anthrathiophenediones in bladder cancer cells. *J. Med.*
5 *Chem.* **2015**, *58*, 5476-5485.
6
7
8
9 62. Shchekotikhin, A.E.; Glazunova, V.A.; Dezhenkova, L.G.; Luzikov, Y.N.; Sinkevich,
10 Y. B.; Kovalenko, L.V.; Buyanov, V.N.; Balzarini, J.; Shtil, A.A.; Preobrazhenskaya,
11 M.N. Synthesis and cytotoxic properties of 4,11-bis[(aminoethyl)amino]anthra[2,3-
12 *b*]thiophene-5,10-diones, novel analogues of antitumor anthracene-9,10-diones. *Bioorg.*
13 *Med. Chem.* **2009**, *17*, 1861-1869.
14
15
16
17
18 63. Tikhomirov, A.S.; Shchekotikhin, A.E.; Preobrazhenskaya, M.N. Methods for the
19 synthesis and modification of linear anthrafurandiones. *Chem. Heterocycl. Compd.*
20 **2014**, *50*, 171-184.
21
22
23
24
25 64. Gronowitz, S. Thiophene and Its Derivatives, Part 2. *The Chemistry of Heterocyclic*
26 *Compounds*; John Wiley & Sons: New York, 1986, Vol. 44.
27
28
29
30
31 65. Tikhomirov, A.S.; Shchekotikhin, A.E.; Lee, Y.H.; Chen, Y.A.; Yeh, C.A.; Tatarskiy,
32 V.V.; Dezhenkova, L.G.; Glazunova, V.A.; Balzarini, J.; Shtil, A.A.; Preobrazhenskaya,
33 M.N.; Chueh P.J. Synthesis and characterization of 4,11-diaminoanthra[2,3-*b*]furan-
34 5,10-diones: tumor cell apoptosis through tNOX-modulated NAD⁺/NADH ratio and
35 SIRT1. *J. Med. Chem.* **2015**, *58*, 9522-9534.
36
37
38
39
40
41 66. Sabatino, G.; Chinol, M.; Paganelli, G.; Papi, S.; Chelli, M.; Leone, G.; Papini, A.M.;
42 De Luca, A.; Ginanneschi, M. A new biotin derivative-DOTA conjugate as a candidate
43 for pretargeted diagnosis and therapy of tumors. *J. Med. Chem.* **2003**, *46*, 3170-3173.
44
45
46
47
48 67. Huang, F.; He, J.; Zhang, Y.; Guo, Y. Synthesis of biotin-AMP conjugate for 5' biotin
49 labeling of RNA through one-step in vitro transcription. *Nat. Protoc.* **2008**, *3*, 1848-
50 1861.
51
52
53
54 68. Isaac-Lam, M.F.; Hammonds, D.M. Biotinylated chlorin and its zinc and indium
55
56
57
58
59
60

- 1
2
3 complexes: synthesis and in vitro biological evaluation for photodynamic therapy.
4
5 *Pharmaceuticals* **2017**, *10*, 41.
6
7 69. Tikhomirov, A.S.; Shchekotikhin, A.E.; Luzikov, Y.N.; Korolev, A.M.;
8
9 Preobrazhenskaya, M.N. Heterocyclic analogs of 5,12-naphthacene-Quinone. 11. A new
10
11 method for preparing 4,11-dimethoxyanthra[2,3-*b*]furan-5,10-dione. *Chem. Heterocycl.*
12
13 *Compd.* **2011**, *47*, 1206-1211.
14
15 70. Phan, A.T. Human telomeric G-quadruplex: structures of DNA and RNA sequences.
16
17 *FEBS J.* **2010**, *277*, 1107–1117.
18
19 71. Cogoi, S.; Shchekotikhin, A.E.; Xodo, L.E. HRAS is silenced by two neighboring G-
20
21 quadruplexes and activated by MAZ, a zinc-finger transcription factor with DNA
22
23 quadruplexes and activated by MAZ, a zinc-finger transcription factor with DNA
24
25 unfolding property. *Nucleic Acids Res.* **2014**, *42*, 8379-8388.
26
27 72. Cogoi, S.; Rapozzi, V.; Cauci, S.; Xodo, L.E. Critical role of hnRNP A1 in activating
28
29 KRAS transcription in pancreatic cancer cells: A molecular mechanism involving G4
30
31 DNA. *Biochim. Biophys. Acta.* **2016**, S0304-4165, 30454-8.
32
33 73. Cogoi, S.; Xodo, L.E. G-quadruplex formation within the promoter of the KRAS
34
35 proto-oncogene and its effect on transcription. *Nucleic Acids Res.* **2006**, *34*, 2536-
36
37 2549.
38
39 74. Cogoi, S.; Zorzet, S.; Rapozzi, V.; Géci, I.; Pedersen, E.B.; Xodo, L.E. MAZ-binding
40
41 G4-decoy with locked nucleic acid and twisted intercalating nucleic acid
42
43 modifications suppresses KRAS in pancreatic cancer cells and delays tumor growth in
44
45 mice. *Nucleic Acids Res.* **2013**, *41*, 4049-4064.
46
47 75. Wlodkovic, D.; Skommer, J.; Darzynkiewicz, Z. Flow cytometry-based apoptosis
48
49 detection. *Methods Mol. Biol.* **2009**, *559*, 1-8.
50
51 76. Biffi, G.; Di Antonio, M.; Tannahill, D.; Balasubramanian, S. Visualization and
52
53 selective chemical targeting of RNA G-quadruplex structures in the cytoplasm of
54
55
56
57
58
59
60

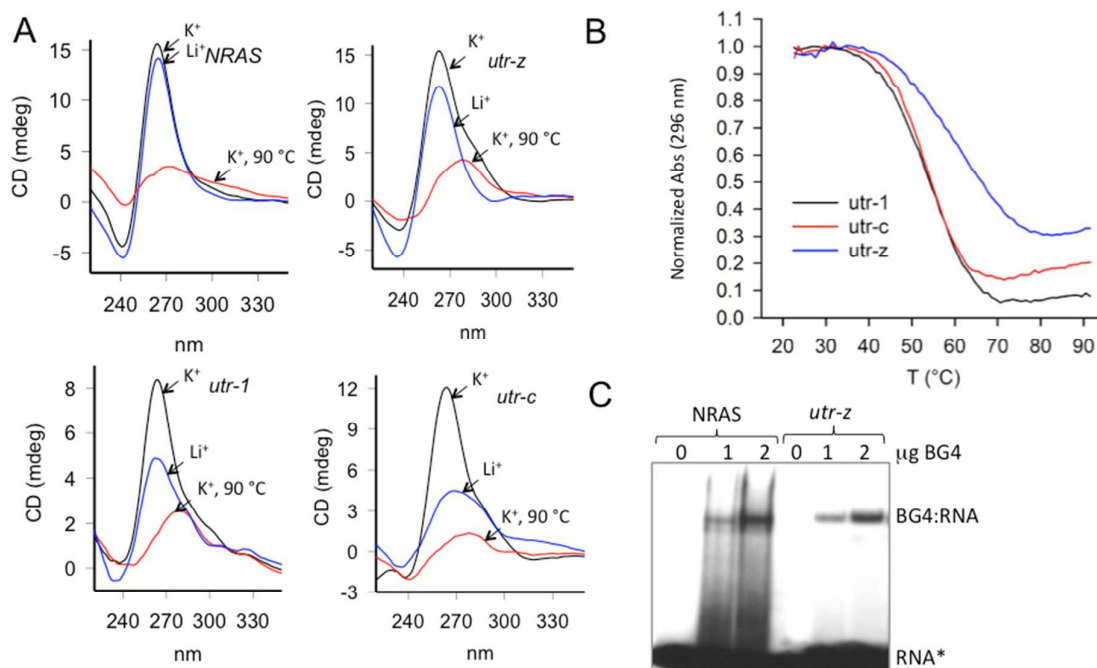


Figure 2. (A) Circular dichroism spectra at 25 and 90 °C of 5 μM *NRAS*, *utr-1*, *utr-c* and *utr-z* RG4s in 50 mM Tris-HCl, pH 7.4, 100 mM KCl (or 100 mM LiCl); for *NRAS* the KCl or LiCl concentration was 20 mM. The spectra were obtained in 0.5 cm cuvette; (B) UV-melting curves of 5 μM *utr-1*, *utr-z* and *utr-c* in 50 mM Na-cacodylate, pH 7.4, 100 mM KCl or LiCl. The curves were obtained measuring the absorbance at 296 nm. The absorbance was normalized with the value at 20 °C; (C) EMSA in 50 mM Tris-HCl, pH 7.4, 100 mM KCl of mixtures containing *NRAS* RG4 and BG4 (lanes 2 and 3 from left) or *utr-z* RG4 and BG4 (lanes 5 and 6 from left). BG4 was used at 1 and 2 μg and the gel was 5 % polyacrylamide in TB.

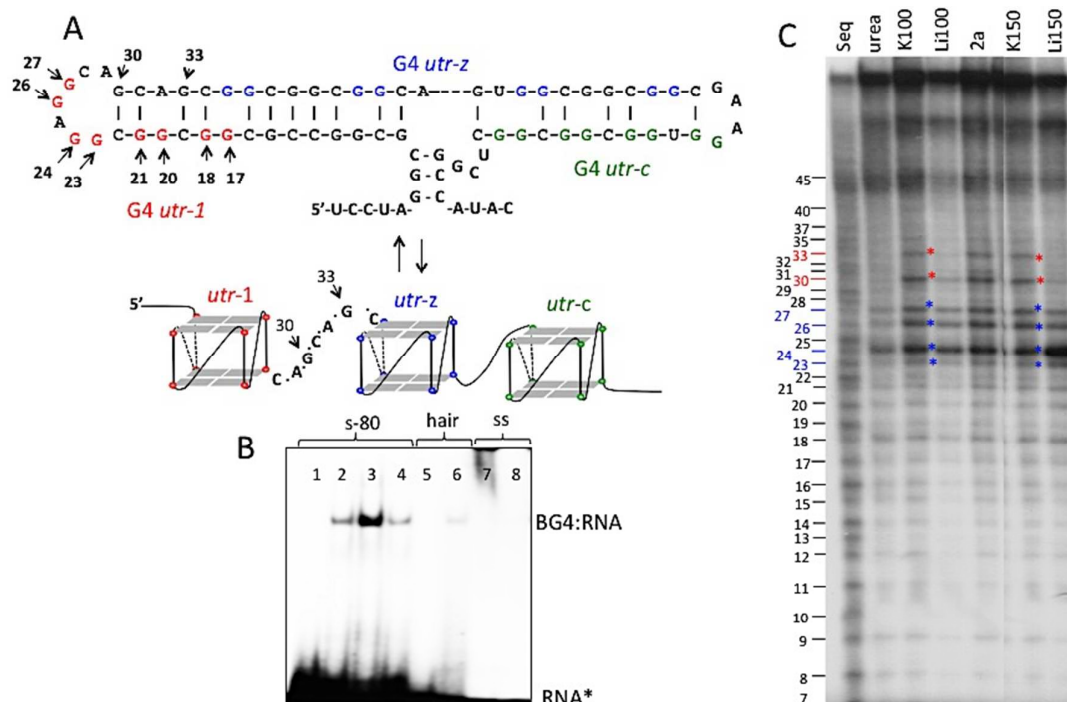


Figure 3. (A) Stem-loop structure of the first 80 nt of *KRAS* 5'-UTR (s-80) given by Mfold. Sequence s-80 is in equilibrium with an alternative structure characterized by 3 non-overlapping G4 RNAs; (B) EMSA in 5% polyacrylamide, TB 1X, of mixtures between BG4 and s-80 or RNA hairpin (hair) 5'-GGCCGCCGCAGUGGCGGCGG or ssRNA 5'-UGUAAACAUCUACACUCAGCU in 50 mM Tris-HCl, pH 7.4, 100 mM KCl (K⁺-buffer) or 100 mM LiCl (Li⁺-buffer). Except mixture 4, all have been prepared in K⁺-buffer. Loading: s-80 (lane 1); s-80 + 1 μg BG4 (lane 2); s-80 + 2 μg BG4 (lane 3); s-80 + 1 μg BG4 in Li⁺-buffer (lane 4); hair (lane 5), hair + 1 μg BG4 (lane 6); ssRNA (lane 7); ssRNA + 1 μg BG4 (lane 8). (C) RNase T1 footprinting of s-80. Loading from left to right: alkaline RNA fragmentation (Seq); RNase T1 reaction in urea (urea), in K⁺-buffer (K100), in Li⁺-buffer (Li100), in K⁺-buffer + **2a** (r=4) to see if the hairpin=G4 equilibrium is shifted by the ligand (**2a**), in K⁺-buffer with 150 mM KCl (K150) in Li⁺-buffer with 150 mM (Li150). The bottom band (band 7) matches the mobility of a 7-mer fragment.

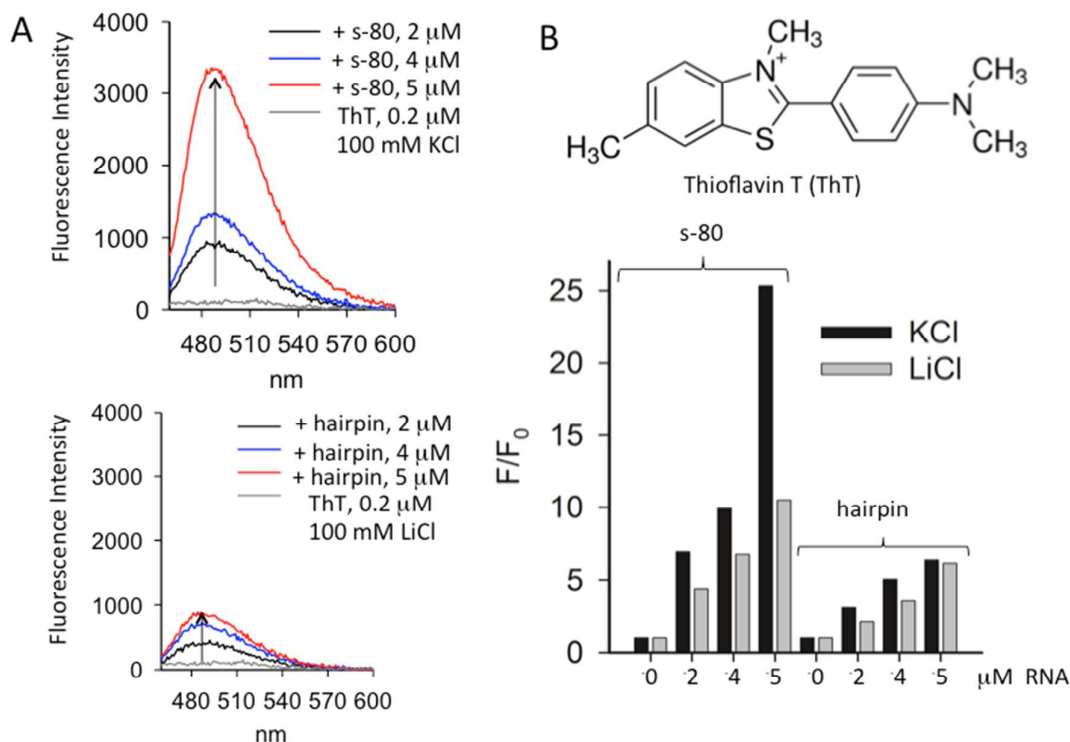


Figure 4. (A) Fluorescence emission spectra in 50 mM Tris-HCl pH 7.4, 100 mM KCl (K^+ -buffer) of 0.2 μ M ThT in the presence of increasing amounts of 80-mer RNA fragment s-80 (top panel) or RNA hairpin 5'-GGCCGCCGAGUGGCGGCGG (bottom panel); (B) Structure of thioflavin T (ThT) and increase of fluorescence quantum yield at 485 nm of ThT following addition of increasing amounts of s-80 or hairpin in K^+ -buffer and Li^+ -buffer (50 mM Tris-HCl pH 7.4, 100 mM LiCl).

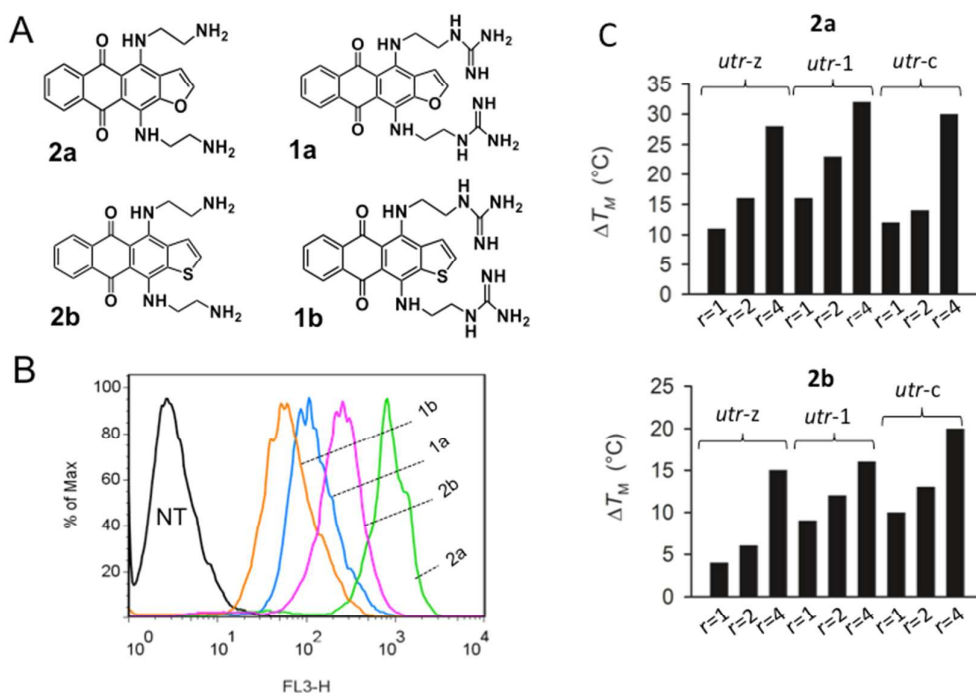


Figure 5. (A) Structures of ATFD **2a**, **1a** and ATPD **2b**, **1b**. Two amine- or guanidine-alkyl side chains have been attached to the ring system of the molecules; (B) Flow cytometry data showing the uptake of 3 μM compounds by Panc-1 cells after an incubation of 4 h. The two alkylamine compounds **2a** and **2b** are taken up more than the guanidine analogues; (C) ΔT_M is the T_M increase of *utr-z*, *utr-1* and *utr-c* G4 RNAs caused by **2a** and **2b** at $r=1$, 2 and 4, in 50 mM Tris-HCl, pH 7.4, 100 mM KCl.

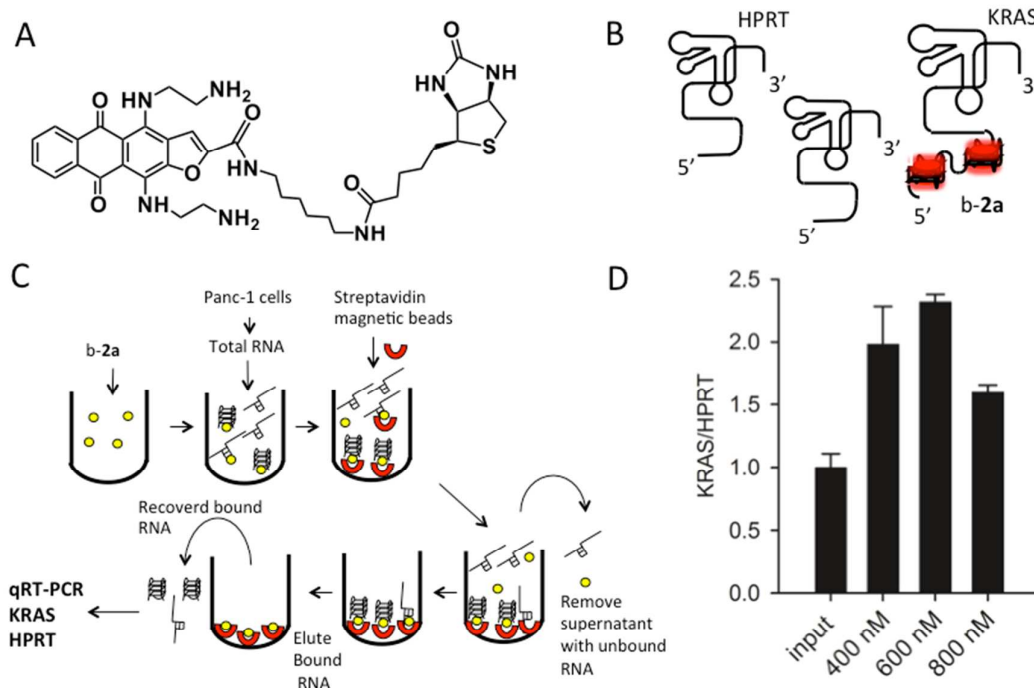


Figure 6. (A) Structure of b-2a conjugated with biotin; (B) Total cellular mRNAs contain *KRAS* mRNA with G4 RNA in the 5'-UTR. G4-RNA is bound by b-2a. *HPRT* is not bound or little bound by b-2a; (C) The streptavidin-biotin pull-down assay: b-2a pulls-down preferentially G4-motif mRNAs. The recovered mRNA was used to determine by RT-qPCR the amounts of *KRAS* and *HPRT* mRNAs; (D) The histograms show the ratio of *KRAS/HPRT* mRNAs in the input, *i.e.* total cellular extract, (fixed to 1) and in the recovered RNA from a total cellular extract treated with increasing amounts of b-2a. An enrichment of *KRAS* over *HPRT* of nearly 3-times was obtained, suggesting that the biotinylated ligands bind to *KRAS* mRNA within the total cellular extract.

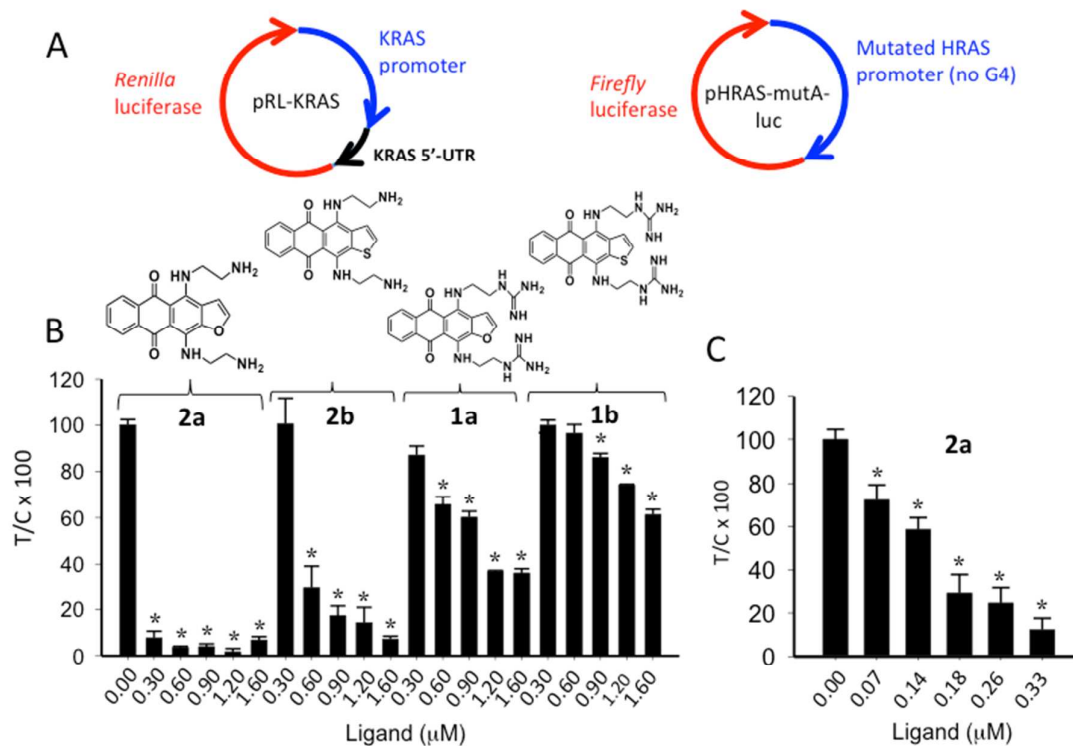


Figure 7. (A, B) Dual luciferase assay showing the effect of compounds **2a**, **2b**, **1a** and **1b** (0-1.6 μM) on *Renilla* luciferase driven by the *KRAS* promoter comprising the 5'-UTR (pRL-KRAS). As reference, we used a plasmid in which *Firefly* luciferase was driven by the *HRAS* promoter mutated in order to abolish its capacity to form quadruplex structures.⁶¹ The assay shows that **2a** strongly inhibit luciferase expression. Also **2b** shows a strong inhibitory activity; (C) Panc-1 cells treated with **2a** at lower concentrations (0-0.33 μM), a dose-response reduction of luciferase is observed. $T = \text{Renilla}/\text{Firefly}$ in treated cells, $C = \text{Renilla}/\text{Firefly}$ in untreated cells. * $P < 0.05$.

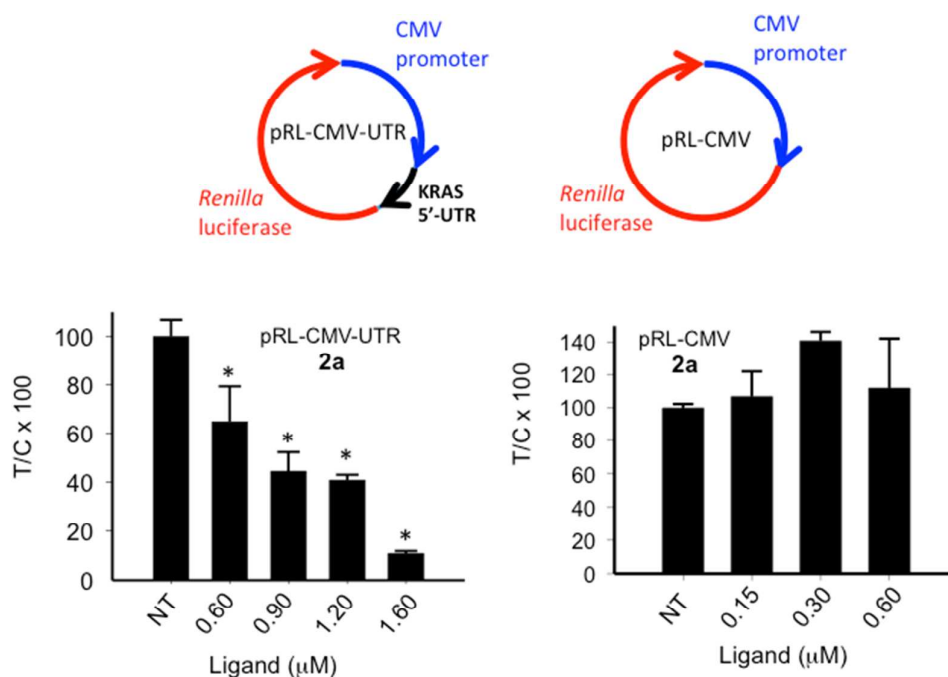


Figure 8. Dual luciferase assay with *Renilla* luciferase plasmid pRL-CMV-UTR or pRL-CMV and *Firefly* luciferase plasmid pHRAS-mutA-luc. Left histograms show a strong dose-response luciferase reduction caused by increasing amounts of **2a** (0-1.6 μM), while the right panel shows that when the *KRAS* 5'-UTR is removed, the luciferase reduction is not observed, suggesting that the inhibitory effect is mediated by 5'-UTR. T=*Renilla*/*Firefly* in treated cells, C=*Renilla*/*Firefly* in untreated cells. * P< 0.05.

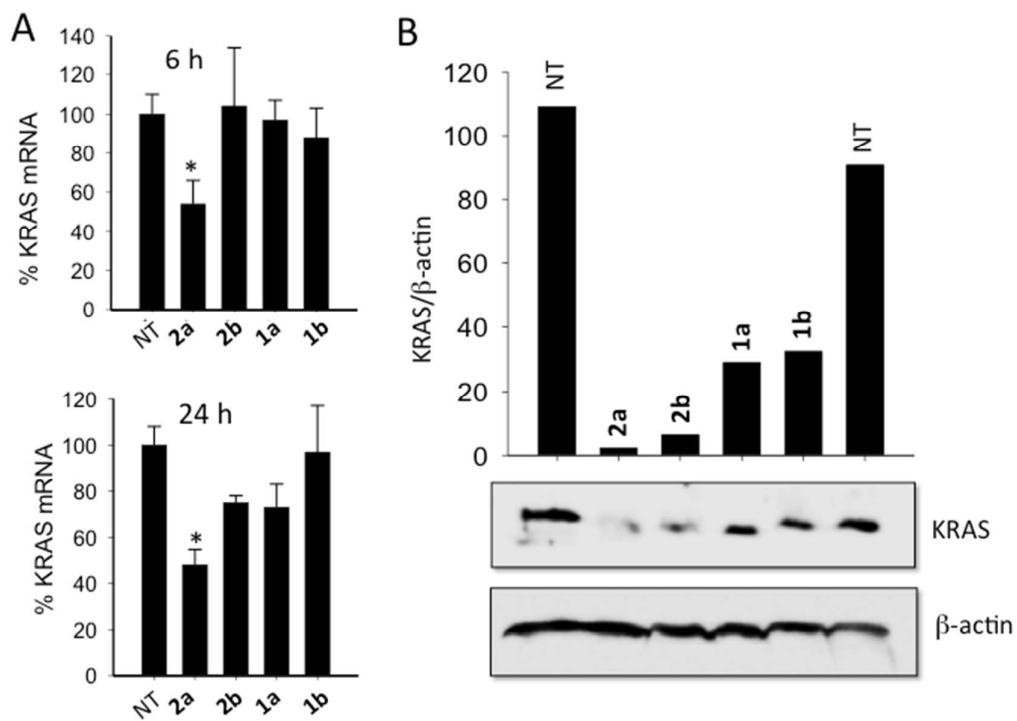


Figure 9. (A) Quantitative RT-PCR of *KRAS* mRNA in Panc-1 cells treated for 6 and 24 h with 1.6 μ M **2a**, **2b**, **1a** and **1b**. Ordinate report the level of *KRAS* mRNA normalized to β 2-microglobulin and HPRT; (B) Western blot determination of *KRAS* protein and β -actin in Panc-1 cells treated with 1.6 μ M **2a**, **2b**, **1a** and **1b** for 48 h. * $P < 0.05$.

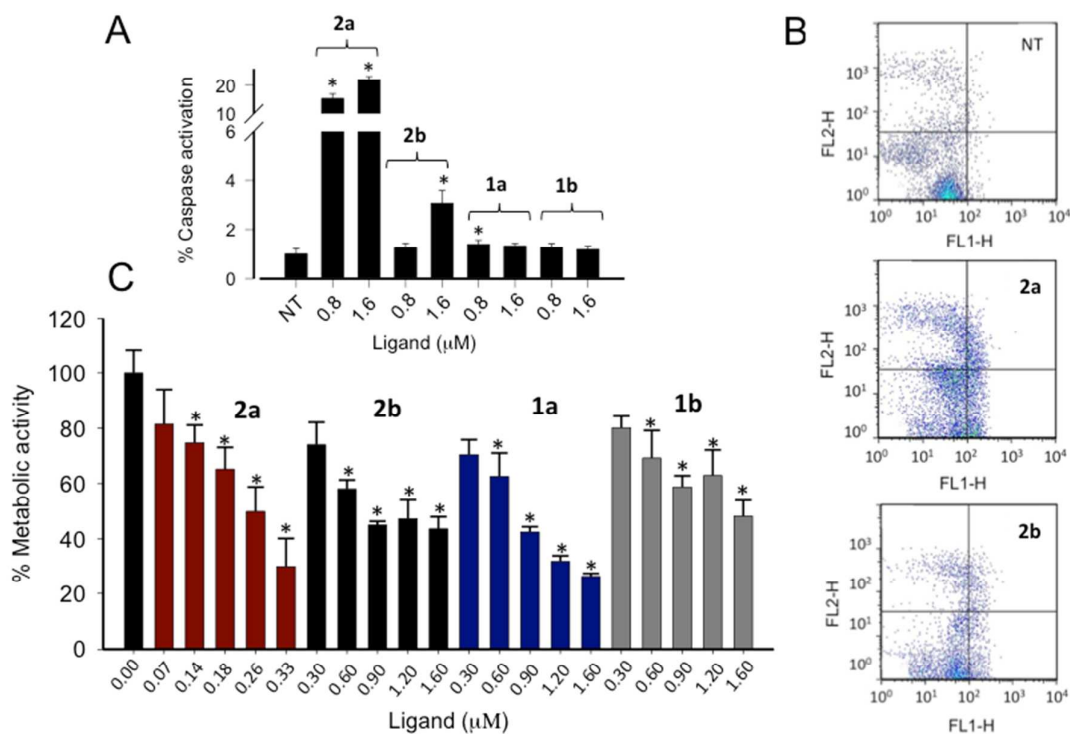


Figure 10. (A) Activation of caspase 3/7 in Panc-1 cells treated with **2a**, **2b**, **1a** and **1b** (0.8 and 1.6 μM). Compounds **2a** and **2b** show the higher activity than the analogues **1a** and **1b**; (B) Annexin-Propidium assay of Panc-1 cells treated for 72 h with **2a** (1.6 μM) and **2b** (1.6 μM); (C) Metabolic activity in Panc-1 cells treated with increasing concentrations of **2a**, **2b**, **1a** and **1b**. Compound **2a** shows the highest activity. * P < 0.05.

Table of Contents graphic

